Design and Analysis of Passively Mode-locked Fiber Lasers Based on Saturable Absorber for Multi-wavelength Applications

Jiang Kai

School of Electrical and Electronic Engineering

A thesis submitted to the Nanyang Technological University
in partial fulfillment of the requirement for the degree of
Doctor of Philosophy

2016

Statement of Originality

I hereby certify that the work embodied in this thesis is the result of original research done by me and has not been submitted for a higher degree to any other University or Institute.

....
Date Jiang Kai

Acknowledgments

First of all, I would like to express my appreciation to Professor. Shum Ping, my supervisor, for his dedicated guidance and encouragement. His enthusiasm and great care for people around him have been inspiring me throughout the whole period of my PhD time.

Secondly, I would like to express special thanks to Dr. Fu Songnian for his endless help and guidance from the beginning of my project. His passion and enthusiasm in research work motivates me to progress in the project. He always likes to discuss project with me and give me some valuable suggestions.

Besides, I want to give thanks to Professor Lin Chinlon, Dr. Tian Xiaolong, Dr. Zhao Luming, Dr. Chen Xueping, Dr. Ouyang Chunmei and all other staffs for their fruitful discussions, suggestions and friendly helps. Many thanks go to all my friends and people in Nanyang Technological University for providing a very friendly and entertaining research environment.

Last I would like to thank all the people who have helped me and affected me in one way or another.

Jiang Kai

July 2016

Abstract

Lasers have been widely used in various fields since the invention of first laser in 1960. Generation of ultra-short optical pulses attracts not only scientists in fundamental researches but also engineers in various applications. Fiber lasers are very promising since they are constructed by inexpensive components (mostly various fibers), highly integrated with flexibly miniaturized cavities, and conveniently collimated output. Recently, mode-locking becomes a routine technique to generate ultra-short optical pulse with pulse width around or below ps. Nowadays, mode-locked laser is considered as the corner stone of ultra-fast optics. More and more researchers around the world are researching on this field.

This thesis first documents the investigation and construction of a passively mode-locked fiber laser based on carbon nanotubes. Passive mode-locking can generate ultra-short optical pulses with fs~ps pulse width. In addition, multiple solitons can be generated in order to increase the repetition rate of pulse trains when a passively mode-locked fiber laser operates under strong pumping. Then I demonstrate the achievement of wavelength-switchable passively harmonic mode-locked fiber laser with low pumping threshold.

To scale up pulse energies extracted directly from fiber oscillators, lasers operating in large normal dispersion regime are preferred. This type of lasers generates typical pulses with large normal chirp and steep spectral edges that are also called dissipative solitons (DSs). It is well known that pulses can be effectively enhanced in energy by lengthening cavity length together with increasing net cavity group velocity dispersion (GVD). Therefore in the middle part of the thesis, I will

propose an all-fiber-integrated erbium-doped dissipative solitons laser with large normal dispersion, which is mode-locked by nonlinear polarization rotation. The pulse energy enhancements are also demonstrated.

Recently ultrafast light sources at 2 μm wavelength region have been widely investigated in recent years due to their eye-safe property, as well as their various scientific applications in the fields of mid-infrared spectrum generation, remote sensing, nonlinear microscopy, medical treatment and free-space communication. In the last part of the thesis, I experimentally demonstrate switchable dual-wavelength mode-locking of thulium-doped fiber laser (TDFL), using single-wall carbon nanotubes as saturable absorber. Due to the cavity birefringence-induced comb filter, switchable mode-locking can be individually realized for the proposed TDFL among three wavelengths. Furthermore, after finely adjusting the intra-cavity birefringence, I am able to demonstrate switchable dual-wavelength mode-locking.

List of Abbreviations

ASE	Amplified Spontaneous Emission
CNT	Carbon Nanotube
FSR	Free Spectral Range
HBF	High Birefringence Fiber
HB-PCF	High Birefringence Photonic Crystal Fiber
LBF	Low Birefringence Fiber
NA	Numerical Aperture
SMF	Single Mode Fiber
SWCNT	Single wall carbon nanotube
PC	Polarization controller
EDF	Er-doped fiber
WDM	Wavelength-division-multiplexing
LD	Laser diode
ESA	Electrical spectrum analyzer
CW	Continuous wave
PML	Passive mode-locking
PMFL	Passive mode-locked fiber laser
FML	Fundamental mode-locking
SMS	Super mode suppression
NLSE	Nonlinear Schröding

List of Figures

Table of Contents

Chapter 1 Introduction

1.1 Background and Motivation

Ultrafast optics is a rapidly growing field. Generation of ultra-short optical pulses attracts not only scientists in fundamental researches but also engineers in various applications. Ultrashort pulses with high intensity make themselves suitable for widespread use in communication, sensing, machining, or medical applications and so on. Various nonlinearities caused by the high pulse intensity also make ultrafast optics an important tool for many branches of science. To date, generation of femtosecond optical pulses is a routine process in two major lasers: bulk solid-state lasers and fiber lasers [1].

A fiber laser is a kind of laser in which the active gain medium is an optical fiber doped with rare-earth ions such as erbium, ytterbium, neodymium, dysprosium, praseodymium, and thulium. They are normally used as doped fiber amplifiers which provide light amplification without lasing. Nowadays, fiber lasers are widely used and researched. Comparing with solid state lasers, they have the advantage of compact, low power consumption and easy maintenance. The fiber laser is becoming an alternative to classic solid state laser [2].

Mode-locking is a mechanism to lock the phase between adjacent longitudinal modes of the laser cavity. Through the locking of such phases, a periodic variation in the laser output will occur. This kind of variation is stable over time. It has a periodicity which is given by the round trip time of the cavity. When

sufficient longitudinal modes are locked together with no phase difference, it can generate a short pulse with significant high peak power and ultra-narrow pulse width [3, 4].

Recently, mode-locking becomes a routine technique to generate ultra-short optical pulse with pulse width around or below ps [5-11]. During the last twenty years, ultra-fast optics has been researched widely. Nowadays researchers have found numerous applications for short pulsed laser systems in areas of fundamental research such as medical and industrial applications. For example, ultra-fast laser systems are used for optical frequency metrology, terahertz generation, two photon spectroscopy and microscopy, and optical coherence tomography [12-18]. In addition, short pulsed laser systems are also used in eye laser surgery, dentist drills and other applications [19-20].In the industry, ultra-fast lasers are used for micro-machining and marking [21]. Nowadays, mode-locked laser is considered as the corner stone of ultra-fast optics. More and more researchers around the world are researching on this field. Generally there are two types of mode-locking which are active mode-locking and passive mode-locking. Normally, in optical communication, active mode-locking is widely used as it can generate optical pulse train with high repetition rate [22].Although passive mode-locking cannot achieve repetition rate as high as active mode-locking, it can generates pulses with shorter pulse width and higher peak power. The generation of solitons in passive mode-locked fiber laser is especially preferred in the field of optical communication.

1.2 Objectives

The initial idea of this work was to design and construct a passive mode locked fiber laser at different wavelength. The aims of my PhD are to learn operation theory of passive mode-locking, then explore the application of passive mode locking at multi-wavelength.

The objectives of this thesis are to design a passive mode locked fiber laser based on saturable absorber and to demonstrate generation of soltions, passive harmonically mode locking, pulse enhancement as well as switchable dual-wavelength mode-locking.

1.3 Thesis Organization

This thesis is organized in the following order:

- Chapter 1: Introduction

  This chapter gives a brief introduction to fiber technology and mode-locking technique.

- Chapter 2: Literature Review

  This chapter provides the fundamental knowledge of laser and passively mode-locked fiber laser.

- Chapter 3: Wavelength-Switchable Passively Harmonically Mode-Locked Fiber Laser

  This chapter demonstrates the achievement of wavelength-switchable passively harmonic mode-locked fiber laser with low pumping threshold.

- Chapter 4: Pulse Energy Enhancement In An All-Fiber Dissipative Soliton

Laser

This chapter demonstrates pulse energy enhancements in all-fiber-integrated erbium-doped dissipative solitons laser with large normal dispersion, which is mode-locked by nonlinear polarization rotation.

- Chapter 5: Switchable Dual-Wavelength Mode-Locking Of Thulium-Doped Fiber Laser Based On Swcnts

  This chapter demonstrates switchable dual-wavelength mode-locking of thulium-doped fiber laser (TDFL), using single-wall carbon nanotubes as saturable absorber.

- Chapter 6: Conclusions

  This chapter gives an overall summary of all the achievements got in this PhD study.

Chapter 2 Fundamentals of Mode-locking

2.1 Introduction

"Laser" refers to Light Amplification by the Stimulated Emission of Radiation. The concept of stimulated emission was introduced by Einstein in 1916. However the first laser was demonstrated as a solid-state laser 40 years later by Theodore Maiman. A laser differs from other sources of light in that it emits light coherently

The frequency locking of three modes which did by Lamb become the trace of invention of Mode-locked laser [23].DiDomenico theoretically predicted mode-locking [24] and Hargrove *et al* demonstrated the first mode-locked laser [25] in 1964. Through internal modulating a laser with acousto-optic modulator, stabilization of amplitude and frequency of the modes in a He-Ne laser was achieved. The laser generate pulses with 56 MHz repetition rate and 2.5 ns pulse width was observed.

In 1965, the first passively mode-locked laser was achieved in a Q-switched laser. Mocker and Collins found that the Q-switched pulse could split into mode-locked pulses in a ruby laser with unstable mode-locking condition. In 1972, Ippen, Shank and Dienes demonstrated the first stable passively mode-locked laser with 1.5ps stable pulse train in a dye laser.

In 1963, Koester and Snitzer demonstrated the first fiber laser [26]. The gain medium is Nd-doped glass fiber. It outputs at 1061nm. After more than 20 years, the first mode-locked fiber laser was demonstrated in 1984.One year later, Mollenauer and Stolen reported the first soliton laser [27]. Later, researchers started intensive research on passively mode-locked fiber laser. Recently, different application areas of passively mode-locked fiber laser have been developed. Different kinds of cavity design realize mode-locked pulses with ultra-low jitter, ultra-short pulse width, high pulse energy in passively mode-locked fiber lasers [28-30].

2.2 Laser Principle

A typical laser contains two important parts: the active medium and optical resonator are shown below:

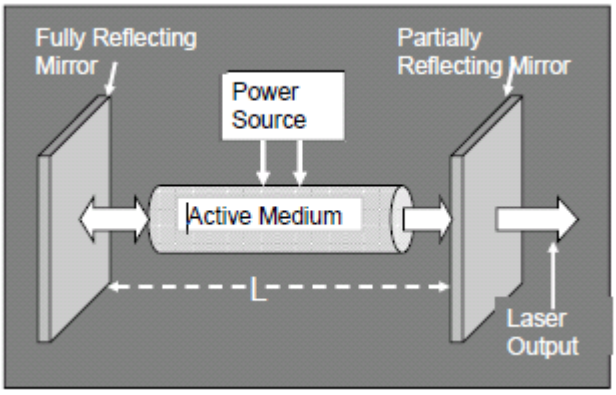

Figure 2-1: Schematic of a laser, L is the cavity length

The active medium provides optical amplification through the process of stimulated emission. When the active medium is pumped by outside power source, some

external photons stimulate the electrons to excite to higher energy level. Figure 2-2 shows the stimulate emission:

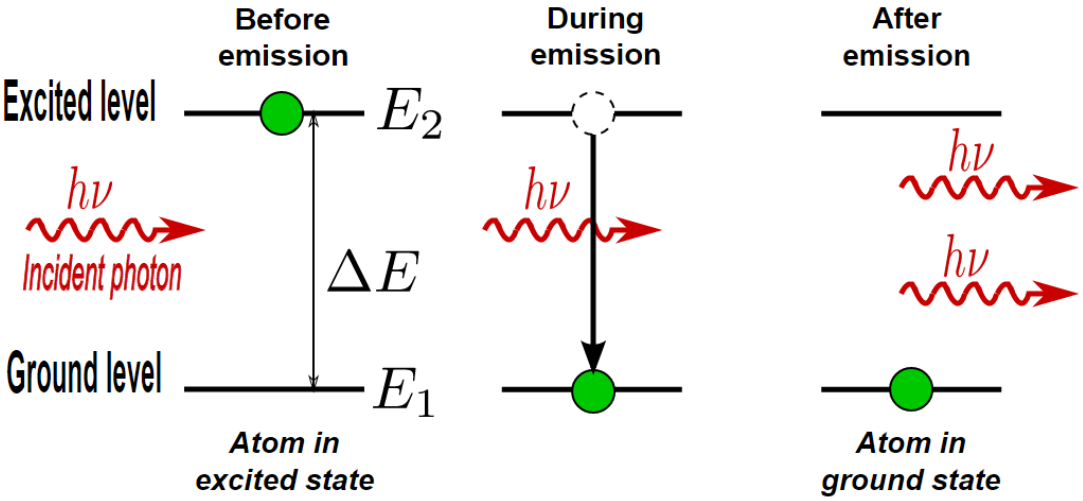

$$E_2 - E_1 = \Delta E = h\nu$$

Figure 2-2: Schematic of stimulated emission [49]

The emitted photon has the energy E_p [69]:

$$E_p = h\nu = \Delta E \qquad \textit{Equation 2-1}$$

h is the Plank constant, v is the frequency of the photon. ΔE is the energy gap between the two energy levels. The emitted photon in stimulated emission has the same phase, wavelength and direction with the incident photon, thus forms optical amplification.

Other than active medium, the optical resonator is essential to provide positive feedback. Normally, the simplest optical resonator contains two reflecting mirrors facing each other which can be seen in figure 2-1. Standing waves are

formed when light bouncing between the mirrors of the cavity. Those generated standing waves will form a discrete set of frequencies which can be seen in figure 2-3. They are called longitudinal modes of the cavity. These modes oscillate in the resonant cavity and have the property of self-regenerating. Destructive interference will suppress other modes.

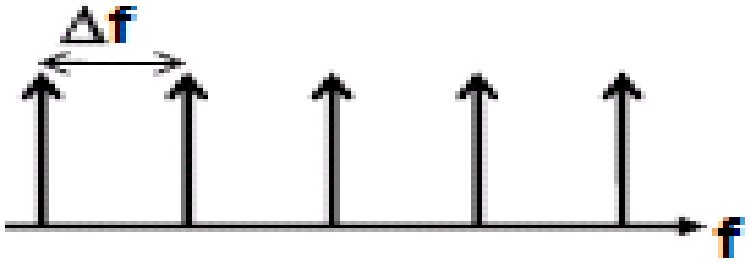

Figure 2-3: Cavity longitude mode structure

In the FP cavity, only frequencies satisfying:

$$2\beta L = 2\pi m \qquad \textit{Equation 2-2}$$

can exist in the cavity.

Where β is the propagation constant and $\beta=2\pi n/\lambda$, n is refractive index of the active region, L is the cavity length, m is positive integer.

2.3 Principle of Mode-Locking

Mode-locking is a technique to generate extreme short pulse. The generated pulses are normally in the order of picoseconds (10^{-12}s) or femtoseconds (10^{-15}s).

The basic principle of mode-locking is to lock the phase between adjacent modes in laser cavity. Through this process, the laser is said to be mode-locked.

Every longitudinal mode operates over a certain bandwidth or range of frequencies. The condition of cavity determines this bandwidth. Normally, this bandwidth is much smaller comparing with the frequency of two adjacent longitude modes. We can treat them as ideal plane wave which was described in equation 2-3:

$$E_j(t) = E_j \exp[i(\omega_j t + \phi_j)] \qquad \textit{Equation 2-3}$$

E_j is the amplitude of electrical field, ω_j is the frequency, ϕ_j is the phase of the j^{th} longitude mode, respectively. Under normal condition, the phases of longitude modes are randomly arranged although the frequencies are fixed according to the optical resonator.

In ideal condition, all longitude modes should have same amplitude E_0, so the output power of laser is equal to:

$$I(t) = |E(t)|^2 = E_0^2 \left| \sum_{j=0}^{N-1} \exp(i\omega_j t) \exp(i\phi_j) \right|^2 \qquad \textit{Equation 2-4}$$

We can see form the above equation, the output power is not fixed due to the change of phase of longitude modes. Once the phase of different longitude modes becomes the same, the above equation becomes to:

$$I(t) = |E(t)|^2 = E_0^2 \left| \sum_{j=0}^{N-1} \exp(i\omega_j t) \exp(i\phi_j) \right|^2$$
$$= E_0^2 \left| \exp(i\phi) \right|^2 \left| \sum_{j=0}^{N-1} \exp(i\omega_j t) \right|^2$$
$$= E_0^2 \left| \sum_{j=0}^{N-1} \exp(i\omega_j t) \right|^2$$
$$= E_0^2 \frac{\sin^2(N\Delta\omega t/2)}{\sin^2(\Delta\omega t/2)}$$

Equation 2-5

In this equation, $\Delta\omega = 2\pi\Delta f$ is the frequency difference between two adjacent longitude modes, N is the number of the longitude modes. Under this condition, the laser generates optical pulse trains with repetition rate equals to Δf, and the pulse period $T = 1/\Delta v$, where Δv is the full width of the gain band.

The method which locks the phase of the longitude modes in a laser is called mode-locking. It can be seen from the above equation, the laser generates short optical pulse train with fixed period. The more the longitudes number, the higher the pulse peak power and the narrower the pulse width.

In a real laser, the amplitudes of different longitude modes are not equal. The amplitude is dominant by the gain profile of the gain medium, as shown in Figure 2.4:

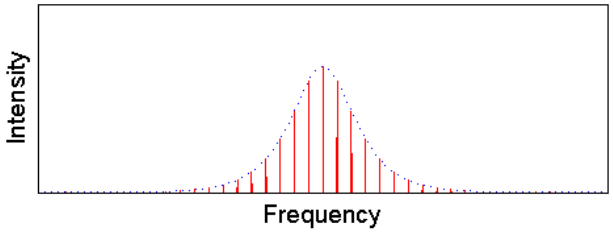

Figure 2-4: Gain profile of active medium

If we treat the gain profile as a Gaussian function, the equation of output power become:

$$I(t) = |E(t)|^2 = \left|\sum_{j=0}^{N-1} E_j \exp(i\omega_j t)\right|^2 \cdot \exp[-\ln 2(\frac{2t}{\Delta t})^2]$$

Equation 2-6

The full width of the half maximum (FWHM) of the pulse is $\Delta t = \frac{2\ln 2}{\pi \Delta v} = \frac{0.441}{\Delta v}$.

The time-bandwidth (TB) product $\Delta t \Delta v = 0.441$ when the phase of each longitude mode is perfectly matched. The time bandwidth product is an important property which was normally used to examine the pulse quality of a mode-locked laser. If a pulse was named "transform limited", that means the phase of different longitude modes are perfectly matched which leads to a TB product equal to 0.441(Gaussian Approximation) or 0.315(secant hyperbolic approximation)

2.4 Active mode-locking and Passive mode-locking

In general, there are two main types of mode-locking mechanisms: active mode-locking and passively mode-locking. In active mode-locking, a modulator modulated by an external signal source shall be applied. The modulator can be either amplitude modulator (AM) or phase modulator (FM). When the modulation frequency is the integral times of the laser cavity frequency, the laser can be mode-

locked and output pulse train synchronized to the external modulation signal. By using harmonic active mode-locking, the repetition rate can be over 1000 times of the fundamental laser frequency and as high as tens of GHz. A bandpass filter (BPF) is always required to stabilize the output. Actively mode-locked lasers can be excellent pulse source for optical communication systems. Figure 2-5 shows a typical actively mode-locked fiber laser

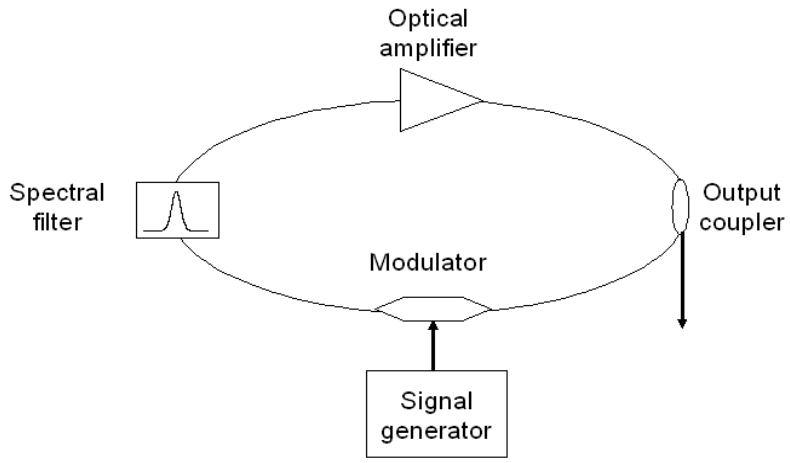

Figure 2-5: Schematic setup of active mode-locked laser

In the passively mode-locked laser, a saturable absorber must be inserted in the laser cavity to start the mode-locking, as shown in Figure 2-6. The saturable absorber is an optical device that exhibits an intensity-dependent transmission. The device behaves differently depending on the intensity of the light passing through it. For passive mode-locking, ideally a saturable absorber will selectively absorb low-intensity light, and transmit light which is of sufficiently high intensity, as shown in Figure 2-7. Such mechanism provides the so called “positive feedback” to the laser cavity which induces higher transmission to light with higher intensity.

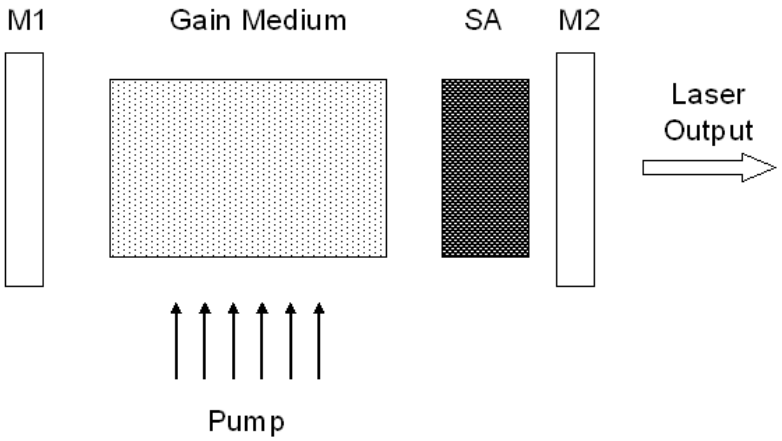

Figure 2-6: Schematic setup of passive mode-locked laser M1: Mirror 1; M2: Partial transmission mirror; SA: saturable absorber,

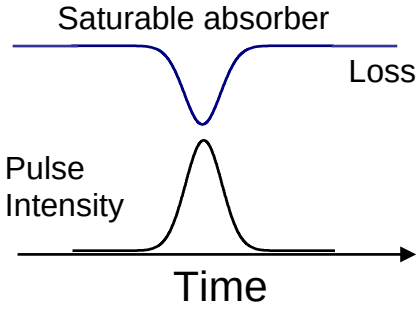

Figure 2-7: The function of saturable absorber

When placed in a laser cavity, a saturable absorber will attenuate low-intensity constant wave light (pulse wings). Because of the random intensity fluctuations experienced by an un-modelocked laser, any random, intense spike will be transmitted preferentially by the saturable absorber. As the light in the cavity oscillates, this process repeats, leading to the selective amplification of the high-intensity spikes, and the absorption of the low-intensity light. After many round

trips, this effect builds up a train of pulses and starts the mode-locking of the laser.

The passive mode-locking can also be understood from the frequency domain. The saturable absorber modulates the light in each roundtrip of the laser cavity with a period of roundtrip time. The modulation frequency equals to the fundamental frequency of the laser thus generate mode-locked pulse train with fundamental repetition rate. Mode-locking based on saturable absorption has the advantage of self-starting and self-sustaining for properly designed laser cavities without any external signal reference.

2.5 Saturable absorber

Saturable absorber is an optical component which reduces losses at high intensity. There are different types of saturable absorbers such as semiconductor saturable absorber mirrors (also called SESAMs), nonlinear polarization rotation (NPR) and nonlinear loop mirrors (NOLMs). Currently, carbon nanotubes are used as saturable absorber.

Semiconductor saturable absorber mirror (SESAM)

A SESAM always consists of a Bragg-mirror on a semiconductor wafer like GaAs, in-corporating materials with an intensity dependent absorption. The saturable absorber layer consists of a semiconductor material with a direct band gap slightly lower than the photon energy. Often GaAs/AlAs is used for the Bragg mir¬rors and InGaAs Quantum Wells for the saturable absorber material. During the absorption electron-hole pairs are created in the film. As the number of photons

increases, more electrons are excited, but as only a finite number of electron-hole pairs can be created, the absorption saturates. The electron-hole pairs recombined non-radiatively, and are after a certain period of time again ready to absorb photons.

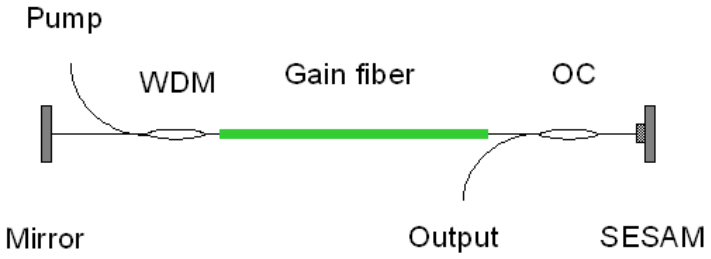

Figure 2-8 Schematic of a SESAM based passively mode-locked fiber laser with a linear cavity. OC: Optical coupler; WDM: Wavelength division multiplexing coupler.

The recovery time should ideally be as small as possible. Recovery times of same orders of magnitude as the pulse duration will cause asymmetric spectra if the pulse is chirped at the impact with the SESAM, and hence strongly affect the pulse dynamics inside the cavity [67]. Larger recovery times can limit the obtainable pulse with from the laser. Because the relaxation time due to the spontaneous photon emission in a semiconductor is about 1 ns, some precautions have to be taken to shorten it drastically. Two technologies are used to introduce lattice defects in the absorber layer for fast non-radiative relaxation of the carriers: low-temperature molecular beam epitaxy (LT-MBE) and ion implantation. The relaxation time can be adjusted by adjusting the growth temperature in case of LT-MBE and the ion dose in case of ion implantation. SESAMs have been known to exhibit a bi-temporal recovery time with the shortest time in the ps or sub-ps range. A bi-temporal recovery time is ideal for mode-locked lasers, because the short recovery time enables short pulses and the longer recovery time is needed to initiate

mode-locking. Figure 2-8 gives a typical SESAM based passively mode-locked fiber laser with a linear laser cavity.

Nonlinear Polarization Rotation (NPR)

One widely used saturable absorber is to use NPR technique by inserting a polarizer into the laser cavity. By correct controlling the polarization state in a fiber with polarization controllers (PCs), the polarizer can provide intensity dependent loss. An optical pulse pass through a polarizer shall be linear polarized at any point in time domain. After one roundtrip in the laser cavity, the fiber nonlinearity will induce NPR effect and the polarization state of the pulse becomes intensity dependent. The polarization state is un-uniformly distributed along the pulse in time domain. By proper setting the PCs in the laser cavity, the pulse peak can achieve highest transmission and the pulse wings which have lower intensity will be suppressed. Therefore, an artificial saturable absorber is formed. Since the saturable absorption effect comes from the Kerr nonlinear effect, the NPR has ultra-fast response time, thus it can always be treated as a device responses instantaneously to the pulse intensity and results in additive pulse limiting (APL) mode-locking [68].

Carbon nanotube

Nowadays, carbon nanotubes especially for single-walled are widely used as saturable absorber. This kind of saturable absorber has some advantages such as ultrafast recovery time, polarization insensitivity, a theoretically high optical damage threshold, mechanical and environmental robustness, chemical stability, and the ability to operate in transmission, reflection, and bidirectional modes. Most

single-walled nanotubes (SWNTs) have a diameter of close to 1 nanometer, and can be many millions of times longer. The structure of a SWNT can be conceptualized by wrapping a one-atom-thick layer of graphite called graphene into a seamless cylinder. The way the graphene sheet is wrapped is represented by a pair of indices (n,m). The integers n and m denote the number of unit vectors along two directions in the honeycomb crystal lattice of graphene. If m = 0, the nanotubes are called zigzag nanotubes, and if n = m, the nanotubes are called armchair nanotubes. Otherwise, they are called chiral. In particular, their band gap can vary from zero to about 2 eV and their electrical conductivity can show metallic or semiconducting behavior. Single-walled nanotubes are likely candidates for miniaturizing electronics

2.6 Soliton

Soliton is a special kind of wave that does not change during propagation. Generally, there are two types of solitons: spatial solitons and temporal solitons. In optics, when refer to solitons it often means temporal soliton. The discovery of solitons can be traced back to 1834 when John Scott Russell describe his wave of translation .In 1989, Drazin and Johnson describe three prosperities of solitons which can be used to define soliton .First of all, and they should have permanent forms. Second, they must localize within a region. Third, they remain unaffected even collision with each other except for a phase shift. Solitons nowadays are widely used in the application of telecommunications which can propagate without degrading the signal to noise ratio between long distances. In optics, solitons are generated due to the balance between the nonlinearity and dispersion in medium.

Chapter 3 WAVELENGTH-SWITCHABLE PASSIVELY HARMONICALLY MODE-LOCKED FIBER LASER

3.1 Introduction

Generation of ultrashort optical pulses with high repetition rate is a rapidly evolving field including much scientific research and various applications, such as optical frequency metrology, high-speed optical sampling, and laser ranging. The rare-earth-doped fiber lasers with the passive mode-locking (PML) technique are promising systems for fulfilling the requirements due to the inherent properties of fibers including a large spectral gain bandwidth, compact size, and easy maintenance. Through harmonic PML techniques [50]–[54], the repetition rate of the pulsed laser can be significantly increased with respect to its cavity fundamental repetition rate.

Various PML techniques, such as nonlinear loop mirror (NOLM) [50], nonlinear polarization rotation (NPR) [54], and semiconductor saturable absorber mirrors (SESAMs) [55], have been successfully demonstrated. However, fiber lasers mode-locked with NPR and NOLM will generally not be environmentally stable. Although SESAMs become a popular choice as a mode-locker, it tends to be damaged, perhaps due to the large modulation depth [56]. Recently, a carbon-nanotube-based saturable absorber (CNT-SA) exhibited unique properties of fast

saturable absorption and wideband wavelength range [56]–[58]. While SESAMs have to be fabricated using sophisticated epitaxial technology, CNT-SAs can be manufactured with relatively simple technology and at low cost. On the other hand, when a fiber laser operates in the anomalous cavity dispersion regime, generally after mode-locking is achieved, soliton shaping of the mode-locked pulses automatically occurs as a result of natural balance between the anomalous cavity dispersion and the fiber nonlinear Kerr effect. Under such a condition, it is possible to generate several pulses per cavity round-trip with a watt-level pumping source. Recently, a soliton erbium-doped fiber laser (EDFL) operating at the 322nd harmonic of the fundamental cavity frequency has been demonstrated with a pumping power above 2 W using NPR techniques [54]. Besides the repetition rate, it is crucial to obtain high supermode suppression (SMS) together with a low timing jitter. The 31st harmonic PML in an Yb-doped soliton fiber laser has been reported with an SMS of 45 dB and a root-mean-square (rms) timing jitter of 6 ps [59].

3.2 Experimental Setup

The SWCNT-based passive mode-locked fiber laser is schematically shown in Figure 3-1. It consists of a self-made fiber-connector-type SWCNT saturable absorber, a polarization controller (PC), an Er-doped fiber (EDF), a 980/1550 nm wavelength-division-multiplexer (WDM), and a fused fiber coupler with 10% output. The polarization-insensitive isolator provides unidirectional operation, while the polarization state of laser in the cavity can be controlled by adjusting the PC. A 980-nm laser diode (LD) is used to provide the pumping power up to 100 mW. An optical spectrum analyzer (OSA) with a resolution of 0.01nm, a 50-GHz

oscilloscope, and a 40 GHz electrical spectrum analyzer (ESA) together with a 40-GHz photo detector are used to monitor the laser output. The SWCNT-polyvinyl alcohol (PVA) is plated on the surface of a fiber-connector [60] and operated in transmission-mode to mode-lock a ring-cavity laser. The highly-concentrated EDF (OFS-EDF150) has a length of 1.8m with normal dispersion of -50 ps/nm/km. The other fibers in cavity are 1m dispersion shifted fiber (DSF) with a dispersion of 0.7 ps/nm/km and 11.2m standard single-mode fiber (SMF) with a dispersion of 17 ps/nm/km, respectively. The total length of cavity is 14 m and the net cavity dispersion is anomalous.

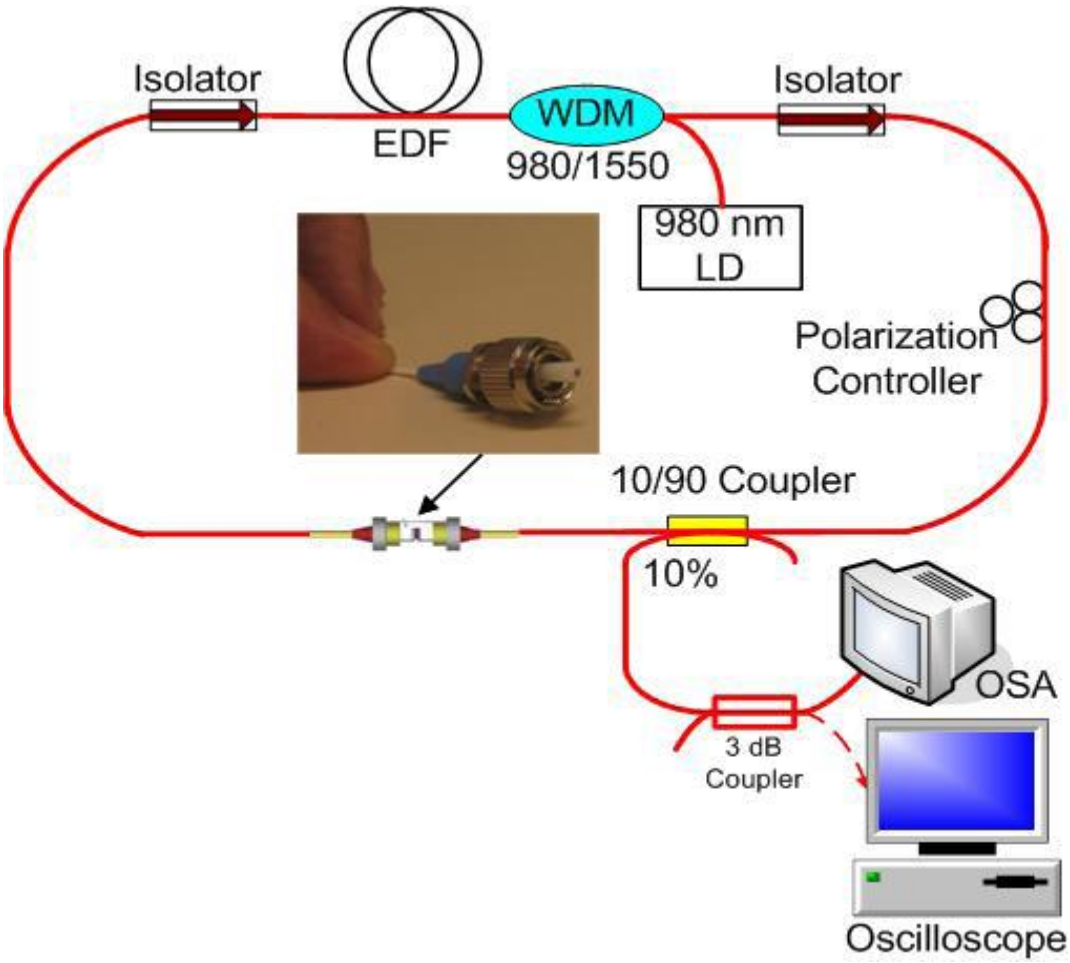

Figure 3-1: Experimental setup of SWCNT-based passively mode-locked fiber laser

3.3 Experiment Results and Discussions

With appropriate settings of the PC, self-started fundamental mode locking at 1554 nm is easily achieved when the pump power is only 12 mW. It is observed that there is a continuous wave (CW) component emitted at 1530nm. After pump power is increased to 60 mw, PML operating at 13th harmonic is achieved by monitoring the temporal waveforms. However the CW component, which is experimentally verified with a measured 3 dB spectral width $\Delta\lambda$ less than 0.04 nm, still appears, as shown in figure 3-2(a).

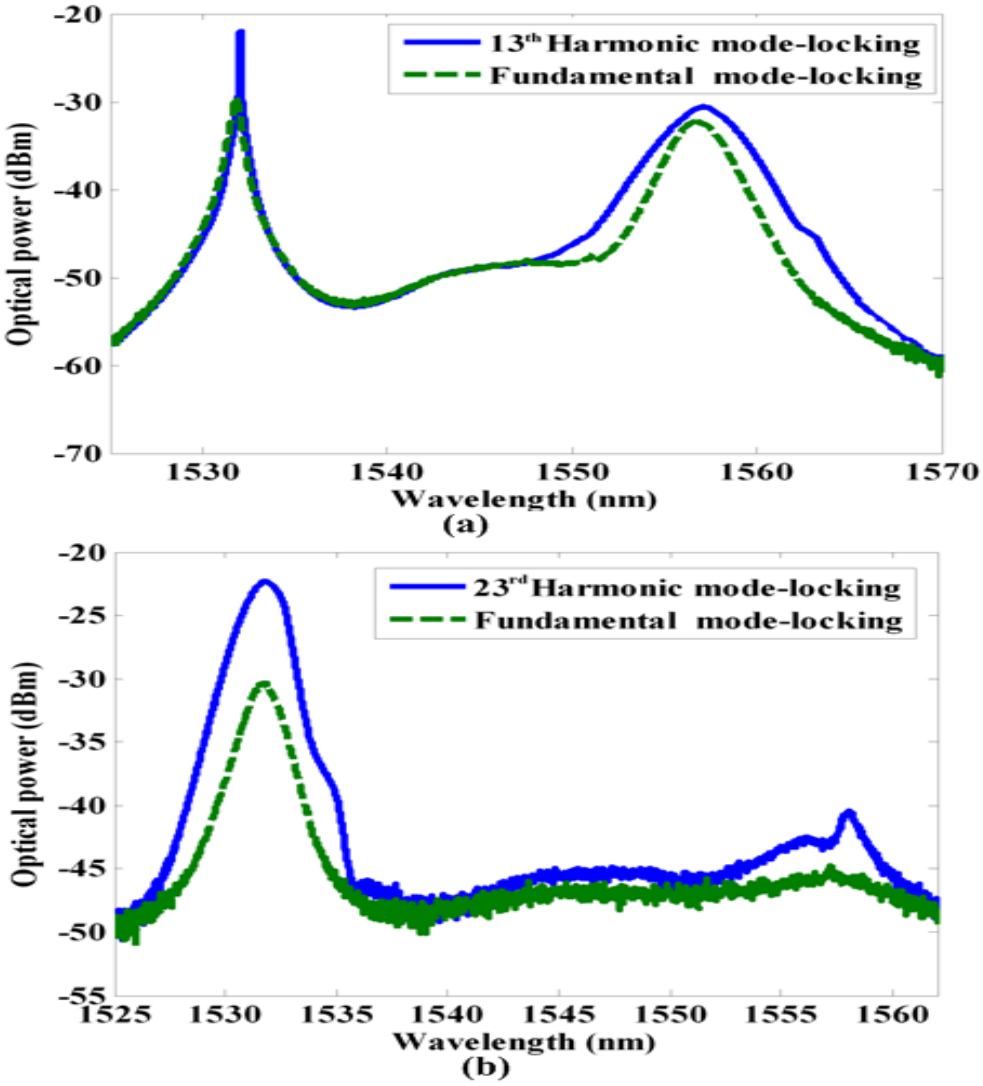

Figure 3-2: Optical spectrum of fiber laser.

When the laser operates at 1554 nm, there always exists a CW component at 1530 nm. The existence of an artificial comb filter from the birefringence of the cavity, together with the gain profile of erbium-doped fiber (EDF), results in a dual-wavelength lasing. However, one lasing operated under CW state due to insufficient pumping power and imperfect polarization state. When the pumping power is experimentally setted to its maximum output (60 mW), an unstable dual-

wavelength passive mode-locking can be observed. In order to achieve a stable fundamental or harmonic passive mode-locking at 1554 nm, I intentionally suppress the 1530 nm lasing to the CW state by adjusting the PC.

Then I reduce the pump power to obtain the fundamental mode-locking at 1554 nm again. Initially, I intend to remove the CW component by varying the PC. However, it is experimentally observed that the wavelength of PML is successfully shifted to 1530nm and less residual component appears at 1554 nm. By increasing the pump power to 60 mW again, PML operation at 23rd harmonic is observed at 1530 nm, as shown in figure 3-2(b). It is experimentally found that the proposed fiber laser always started mode-locking at the same pump power level, and immediately after the fundamental mode-locking multiple solitons are formed in the cavity. If the laser cavity has generated solitons already, after increasing the pump power and adjusting PC, new solitons are observed one by one in the cavity.

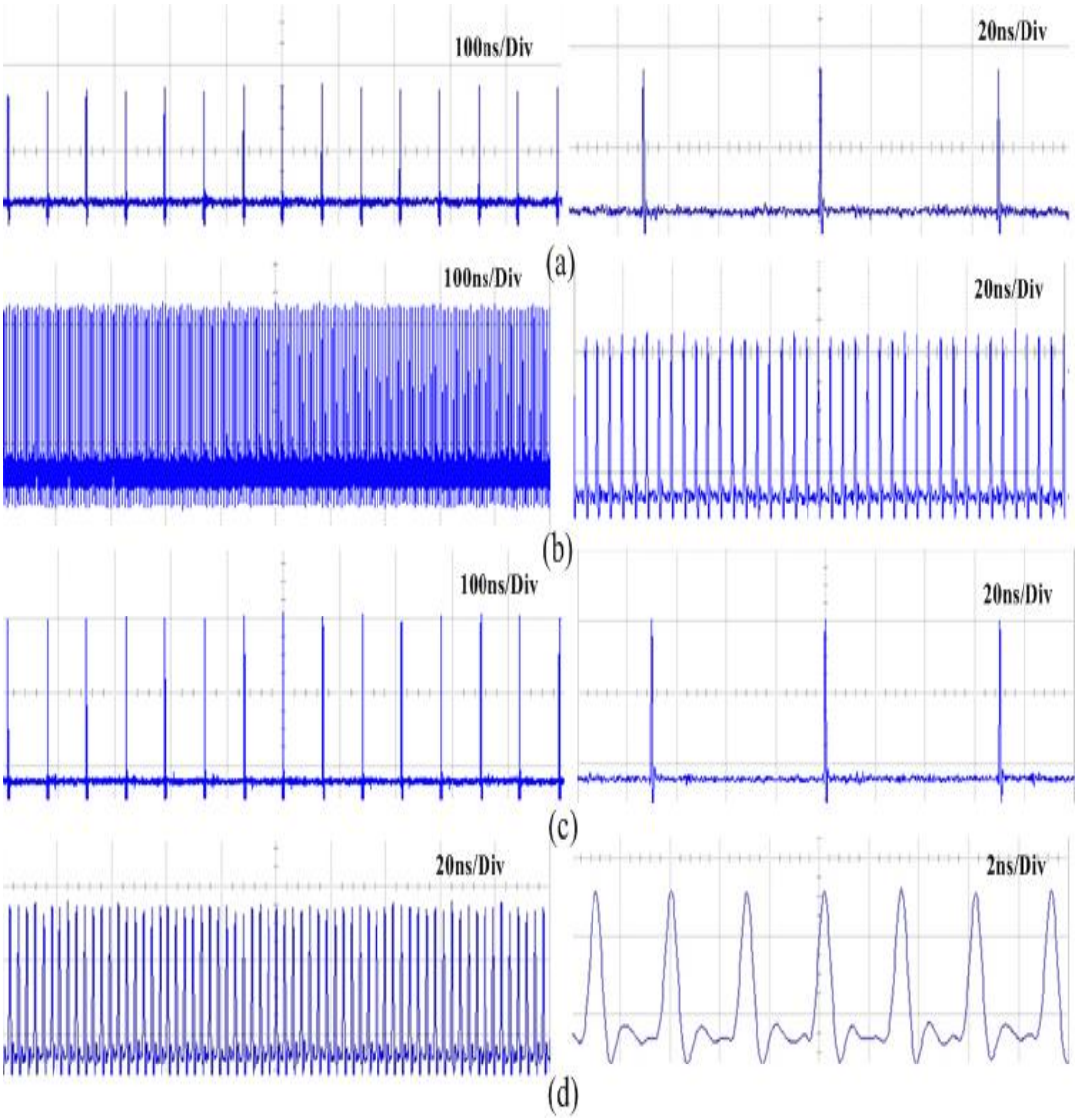

Figure 3-3 Temporal waveforms of fiber laser. (a) Fundamental PML at 1554nm, (b) Harmonic FML at 1554nm, (c) Fundamental PML at 1530nm, (d) Harmonic FML at 1530nm

Figure 3-3 (a) shows the temporal waveform of fundamental PML at 1554 nm, when pump power is 12 mw. The repetition rate of pulses is the fundamental cavity repetition rate, 14.28 MHz, corresponding to the pulse separation of about 70 ns. When the power is increase to 60 mw, the repetition rate of pulses becomes 185.64 MHz which is 13 times of fundamental cavity repetition rate, as shown in figure 3-3 (b). At this state, decreasing the pump power to 12 mw and adjusting the

PC, it is observed that the fundamental PML shifts to 1530 nm and the laser generates pulse trains with a repetition rate of 14.28 MHz .Further increasing the pump power to 60mw and adjusting the PC, the distribution of 23 solitons is observed uniform, as shown in figure 3-3 (d). Thus the laser is passively mode-locked at the 23rd harmonic with a repetition rate of 328.44 MHz. The PML is self-started if the pump power is switched off/on.

Usually, the SMS is used to evaluate the passive harmonic mode-locking by analysis the RF spectrum of the output pulse. The RF spectra of fundamental mode-locking and harmonic mode-locking at individual wavelength are measured, as shown in figure 3-4 to 3-7:

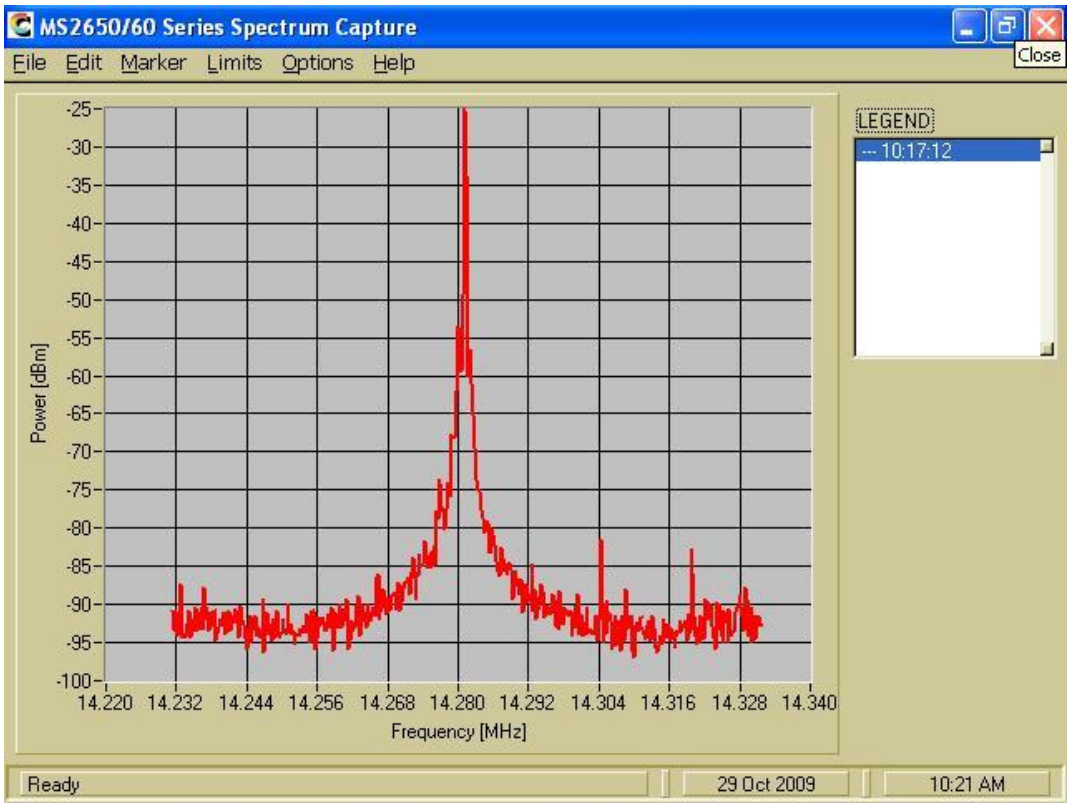

Figure 3-4: RF spectrum of fundamental PML at 1554 nm

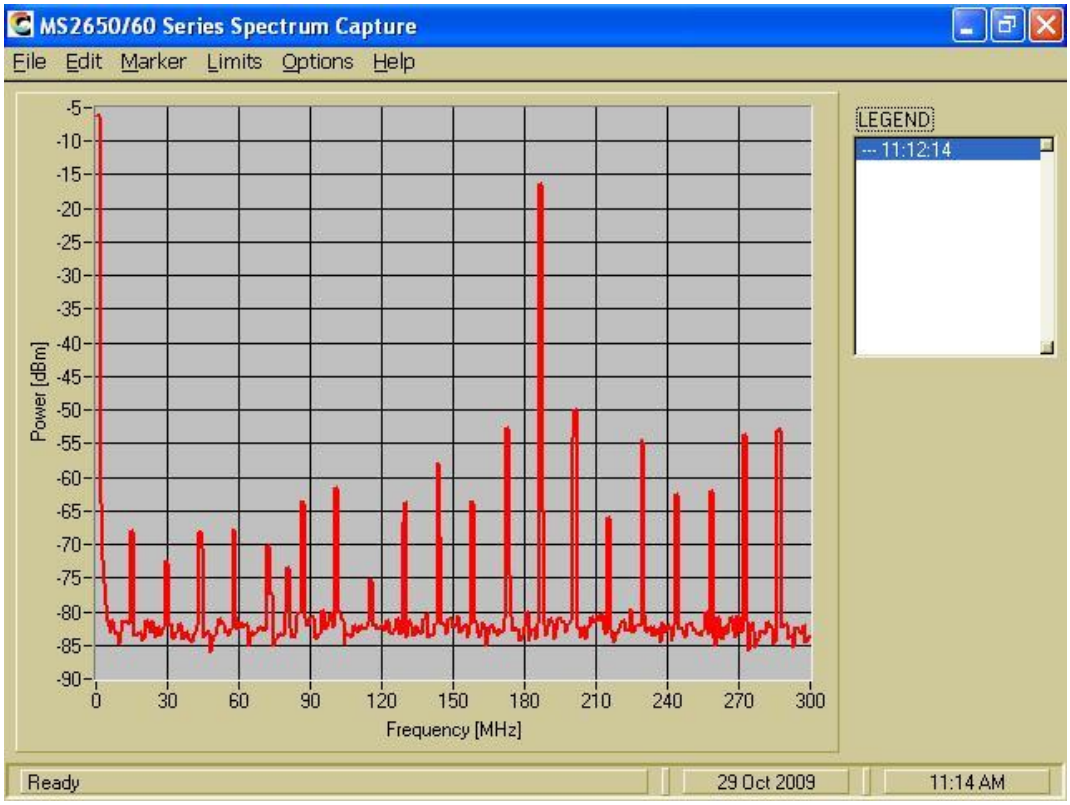

Figure 3-5: RF spectrum of harmonic PML at 1554 nm

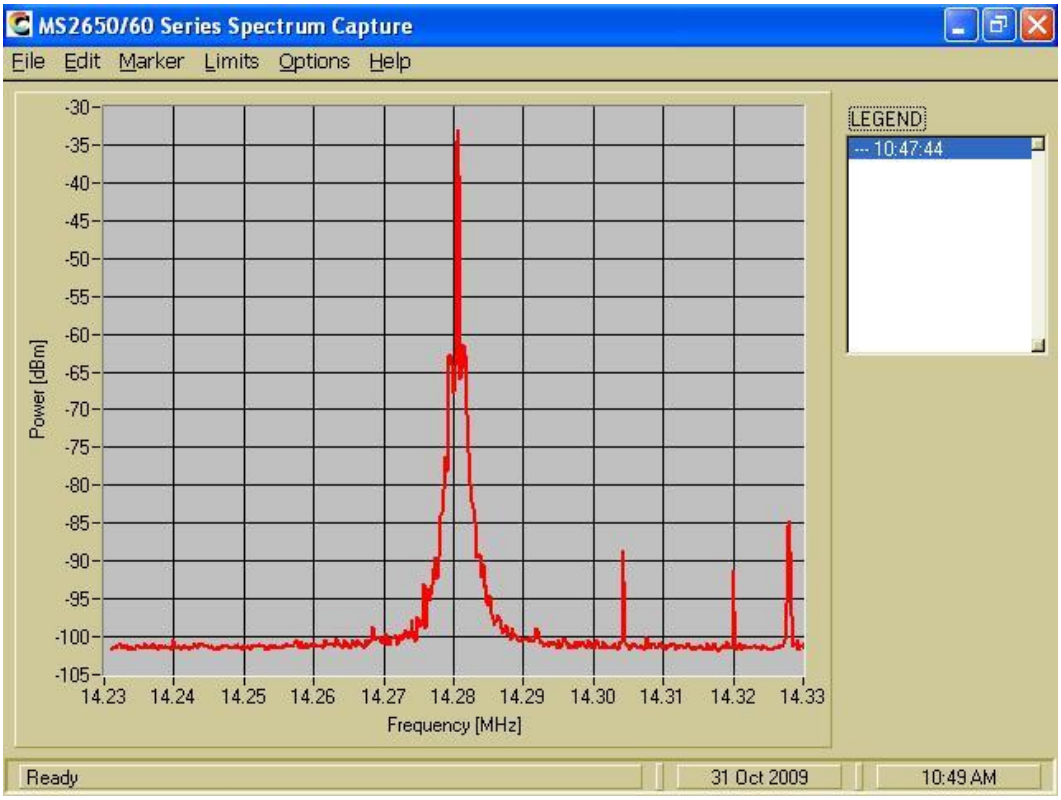

Figure 3-6: RF spectrum of fundamental PML at 1530 nm

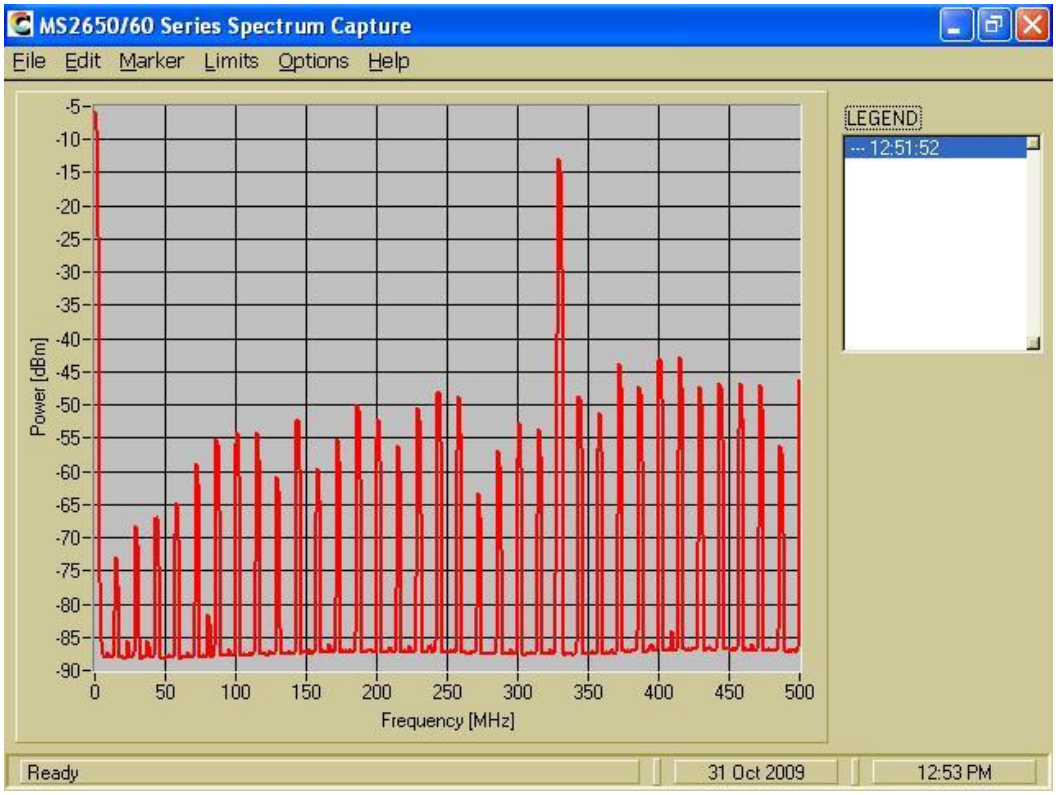

Figure 3-7: RF spectrum of harmonic PML at 1530 nm

It can be seen from figure 3-4 and 3-6 that the fiber laser is mode-locked at fundamental repetition rate of 14.28 MHz. However one is mode-locked at 1554nm while the other one is mode-locked at 1530nm. The main reason for this is the special property of EDF which has two absorption peaks at 1530nm and 1560nm. From figure 3-5 and figure 3-7, the fiber laser is harmonic passively mode-locked at 1554nm and 1530nm respectively. For 1554nm, the generated output pulses have a repetition rate of 185.64 MHz while they have a repetition rate of 328.44 MHz at 1530nm. Normally when I examine the quality of a mode-locked fiber laser, I will look at the SMS from the RF spectrum. It is clearly shown that for both case the SMS is deduced larger than 30dB for each wavelength.

The maximum harmonic (23rd) of fundamental cavity repetition rate at 1530nm is different from the one (13th) at 1554nm. It is due to the same pump power at two different wavelengths. First of all, I get the result of 13^{th} harmonic mode-locking at 1554nm when the pump power is 60mw. Then I keep the 60mw and adjust the polarization controller to get the result of 23^{rd} harmonic mode-locking at 1530nm. The harmonic number "13^{th}" and "23^{rd}" of mode-locking are determined by the pulse energy of fundamental soliton at each wavelength. Since our fiber laser operated at the anomalous cavity dispersion regime, the pulse width and the cavity dispersion are different at 1530 nm and 1554 nm. Thus, the pulse energy of fundamental soliton is different at each wavelength. Under the same pumping power, the achievable maximum number of soliton is different at different wavelength. Since the passive harmonic mode-locking is achieved by the multiple soliton generation and soliton energy quantization effect, increasing the pumping power will not increase the pulse energy of fundamental soliton, but generate new solitons one by one in the cavity. Thus, multiple solitons are formed in the cavity and the order of harmonic mode-locking is different under the same pumping power, due to the different soliton energy at each wavelength. In the experiment, I can realize the same harmonic number of mode-locking at either 1554 nm or 1530 nm, in case I vary the pumping power, respectively. The existence of an artificial comb filter from the birefringence of the cavity, together with the gain profile of erbium-doped fiber (EDF), results in a wavelength-switchable lasing. Thus, the emission wavelength of harmonic passive mode-locking can be experimentally switched by only adjusting the laser polarization in the cavity.

Finally, I characterize the pulse emitted at 1530 nm in details. Figure 3-8 shows the autocorrelation trace of the pulses mode-locked at 23rd harmonic. A good fit is obtained by using a $sech^2$-pulse shape, yielding a full width at half-maximum (FWHM) of 1.3 ps. Since the optical spectral bandwidth at half-maximum is $\Delta\lambda$=1.77nm, the time-bandwidth product is 0.316, indicating that the pulses are almost transform-limited.

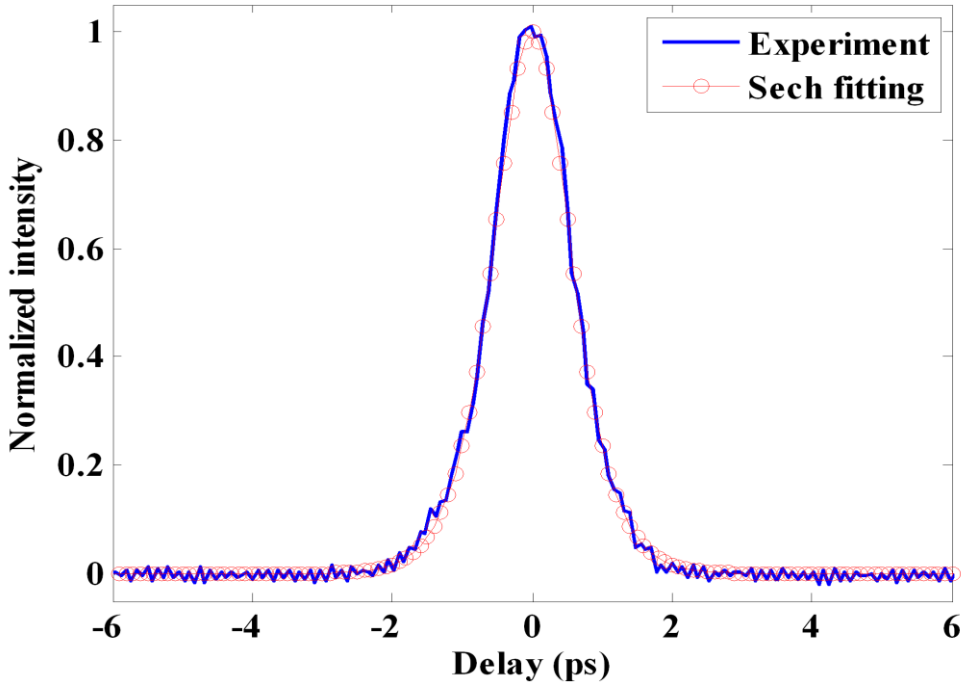

Figure 3-8: Autocorrelation trace and a $sech^2$ fitting.

I have also measured the average output power when the fiber laser is passively mode-locked at fundamental repetition rate of 14.28 MHz at 1530nm. With pumping power of 12mW, the average output power measured at the 10% port of output coupler is about 35 μW, corresponding to 2.45 pJ pulse energy. After increasing the pumping power to 60 mW, the 23rd harmonic mode-locking is

achieved at 1530 nm. The average output power of pulses with a repetition rate of 328.44 MHz is measured about 1.16 mW, corresponding to 3.53 pJ pulse energy. In addition, I also measure the pulse duration of the pulses mode-locked at the 13th harmonic at 1554 nm. The full width at half-maximum (FWHM) of 1.0 ps is obtained after fitting with a sech^2-pulse profile. Since the 3 dB spectral width is 3.9 nm, the time-bandwidth product is 0.316(the same as 1530nm).

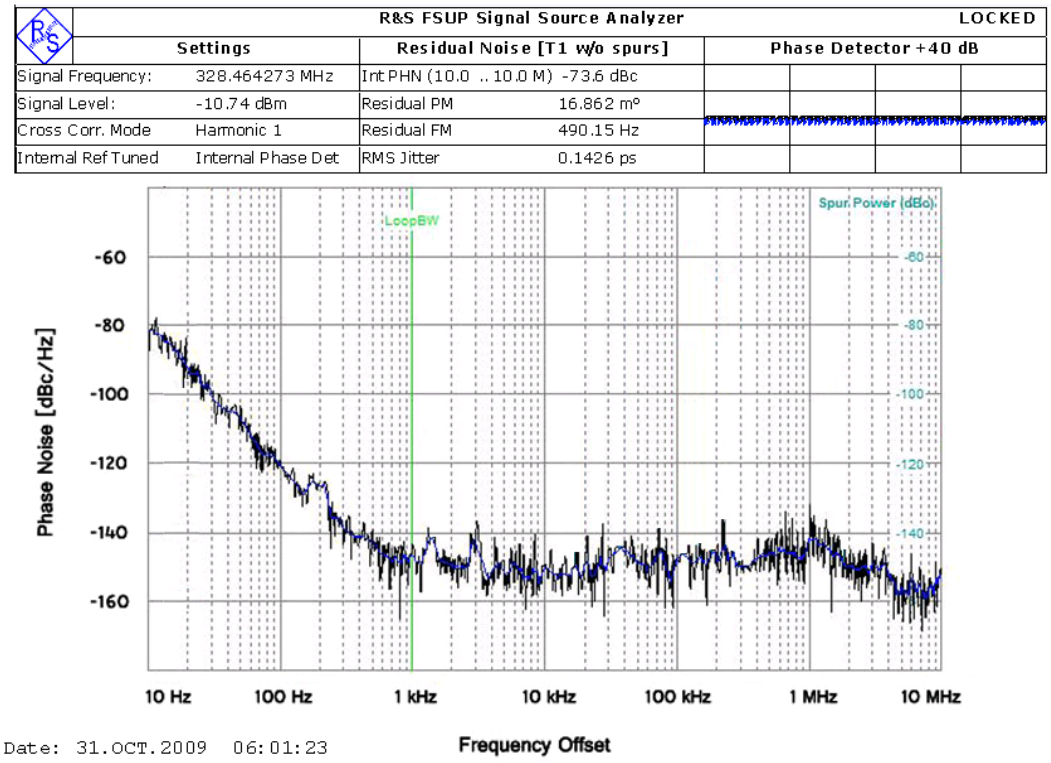

Figure 3-9: Measured timing-jitter of output pulse

During experiment, I also use with R&S FSUP26 signal source analyzer to measure the phase noise of pulses with a repetition rate of 328.44 MHz(which is the highest in this whole experiment, in this experiment I focus on the measurement at 1530nm

only). The timing jitter integrated from 100 Hz to 10 MHz is 142.6 fs which is shown in Figure 3-9.

3.4 Chapter summary

In this chapter, I have experimentally demonstrated a wavelength-switchable passive harmonically mode-locked fiber laser with low pumping threshold using SWCNT. With the help of SWCNT, both multiple soliton generation at different wavelength and low pumping threshold has been achieved simultaneously. When the 980 nm laser diode provides a 60 mW pumping, the fiber laser is passively mode-locked at either 23rd harmonic at 1530 nm or 13th harmonic at 1554 nm by setting different polarization in the cavity, respectively. The measured SMS of each wavelength is more than 30 dB. The pulses at 1530 nm are characterized with a repetition rate of 328.44 MHz, a transform-limited pulse width of 1.3 ps, and a timing jitter of 142.6 fs.

Chapter 4 PULSE ENERGY ENHANCEMENT IN AN ALL-FIBER DISSIPATIVE SOLITON LASER

4.1 Introduction

Fiber pulsed lasers with the advantages of simple design, low cost and high stability have been proved to be strong competitor with solid state lasers and attracted extensive attention in the last few years [34–35]. To scale up pulse energies extracted directly from fiber oscillators, lasers operating in large normal dispersion regime are preferred. This type of lasers generates typical pulses with large normal chirp and steep spectral edges that are also called dissipative solitons (DSs). It has been shown that spectral filtering plays a curial role in DS formation in fiber lasers with large normal dispersion. Recently, Chichkov et al. demonstrated an all-normal-dispersion (ANDi) fiber laser with pulse energies of 20 nJ emitting at 1.5 μm region with erbium-doped fiber (EDF) as a gain medium. In this fiber laser, a bulk birefringent filter was used to dominate the DS pulse shaping and stabilize the laser operation [61]. In the same year, Liu et al. reported a compact all-fiber EDF laser with large normal dispersion. By nonlinear polarization rotation the laser produced pulses with 8 nJ of the pulse energy [33].

It is well known that pulses can be effectively enhanced in energy by lengthening cavity length together with increasing net cavity group velocity dispersion (GVD).

4.2 Experimental Setup

The experimental setup is shown in figure 4-1. The laser oscillator is made of a polarization-independent isolator, a fiber based polarizer, two sets of polarization controllers (PCs), a wavelength division multiplexer (WDM) combining the pump and signal at 976nm and 1550nm, a 15-m-long EDF with GVD of 28 ps^2/km and a fused coupler with 70% output coupling ratio. The polarization state of light in the laser cavity can be controlled by adjusting the PCs, which works together with the polarizer suppressing one polarization to achieve mode-locking by NPR. The pigtailed fiber of the WDM is 1.5-m-long HI1060 Flex fiber with GVD of 20 ps^2/km. The polarizer and the isolator are made with standard single mode fiber (SMF) with GVD of -22 ps^2/km, and the total pigtailed fiber is 1.5m long. The two sets of PCs and the output coupler are made of 7-m-long dispersion compensation fiber (DCF) with GVD of 5.2 ps^2/km. The ring cavity also contains a 64-m-long DCF to increase the cavity length and net cavity dispersion. The total length of the laser oscillator is 89 m resulting in a ~2.3 MHz fundamental repetition rate and the net cavity GVD is about 0.78 ps^2.

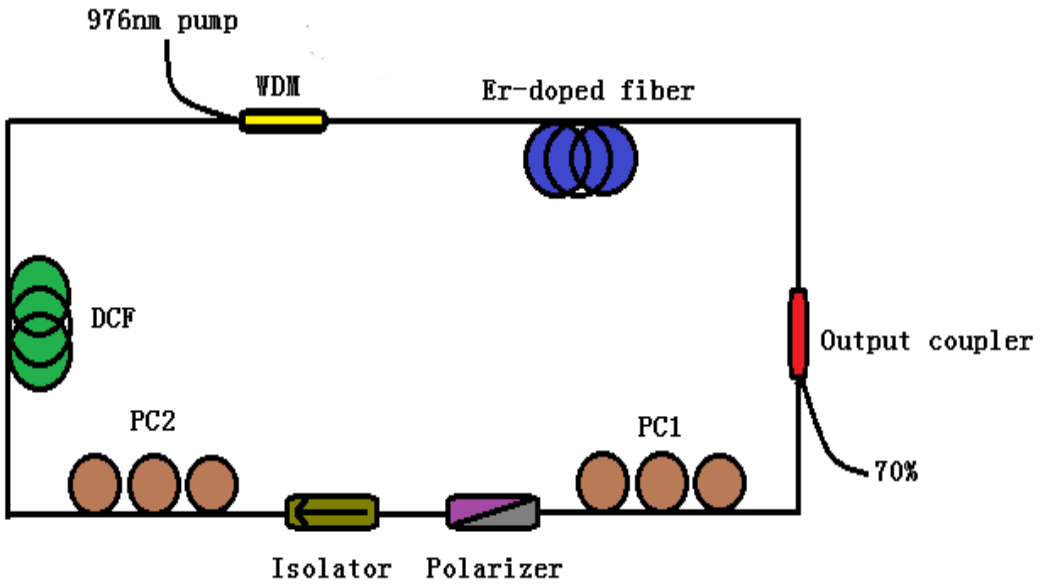

Figure 4-1: Experimental setup of the large normal dispersion EDF laser mode-locked using nonlinear polarization rotation. (DCF: dispersion compensation fiber, PC: polarization controller, WDM: wavelength division multiplexer.)

4.3 Experiment Results and Discussions

Initially, the 64-m-long DCF was not added into the laser cavity and, therefore, the total cavity length in this case is about 25 m and the net cavity GVD is ~0.45 ps^2. By appropriately adjusting the PCs within the cavity, self-starting mode-locking and single-pulse operation were achieved when the pump power was beyond a threshold value of 88 mW. After mode-locking, the laser generated stable pulse trains with the fundamental cavity repetition rate of about 8.3 MHz. From the measured radio frequency (rf) spectrum, a signal-to-noise ratio up to 80 dB was achieved, indicating that stable mode-locking was realized. When the pump power was increased above 280 mW, multi-pulse operation was observed. Figure 4-2 (a) shows the optical spectrum of the output pulse at pump power of 280 mW. Obviously, the optical spectrum of the pulse has the characteristic steep spectral

edges of DSs [31, 32]. It has an edge-to-edge spectral width of 23 nm, centered at 1561 nm.

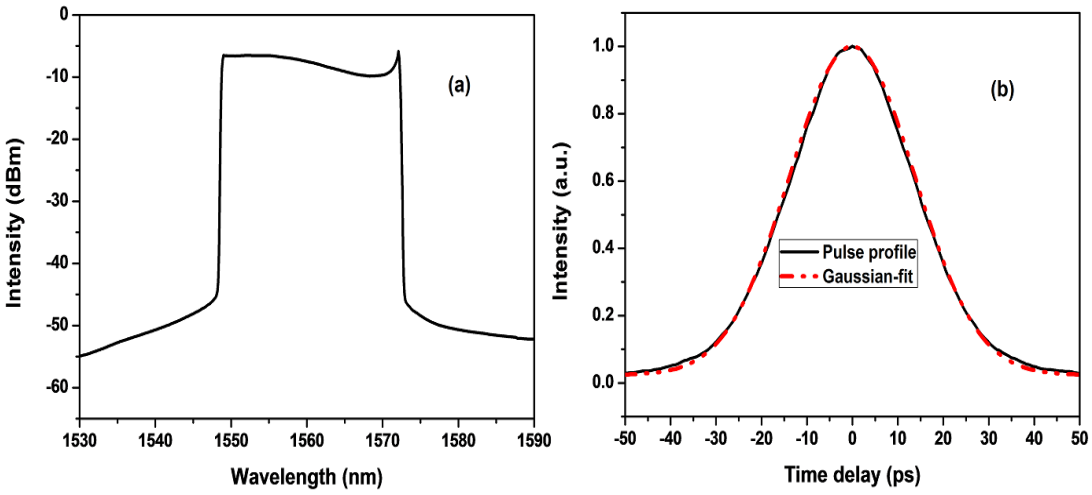

Figure 4-2: (a) Optical spectrum of the output pulse. (b)Autocorrelation trace of the chirped pulse.

The measured autocorrelation trace is shown in Figure 4-2 (b). It shows that the autocorrelation trace has a full width at half maximum (FWHM) of about 33 ps, corresponding to 23 ps of pulse duration due to its Gaussian profile. The time-bandwidth product is 66. The measured average output power is 48.4 mW, thus the calculated pulse energy is up to 5.9 nJ.

When the 64-m-long DCF was added into the laser cavity, the total cavity length was increased to 89 m. Once the PCs were under proper settings, the laser was self-started and single pulse operation was achieved when the pump power was above 62 mW. The fundamental repetition rate was observed to be 2.3 MHz. When the pump power was in the range of 62 mW to 100 mW, the laser operated on the single pulse state. With the pump power at 100 mW, the output was characterized with a 20-GHz real time oscilloscope and an autocorrelator. The measured

oscilloscope trace and the rf spectrum were shown in Figure 4-3. The period of the pulse trains is 435ns (see Figure 4-3(a)) which agrees well with the repetition rate of 2.3MHz. Figure 4-3(b) shows the measured rf spectrum of the output pulse trains. It was measured by a 2-GHz photodetector and a signal-source analyzer (SSA, Rohde and Schwarz FSUP26). The signal-to-noise ratio is up to 80dB at a 300Hz resolution bandwidth, which indicates stable single pulse operation is attained.

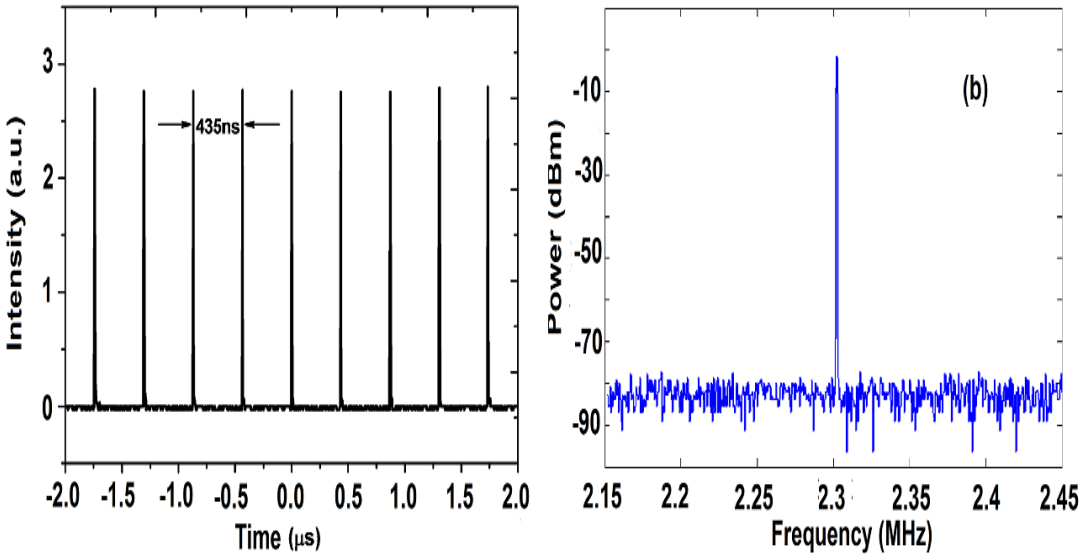

Figure 4-3: (a) Oscilloscope trace of the output pulse trains. (b) rf spectrum of the output pulse trains

Figure 4-4(a) shows the output optical spectra at different pump power. It can be seen that the output optical spectra have the characteristic steep edges, indicating that DSs are formed in this long laser cavity with strong net normal dispersion. With the pump power increasing from 62 mW to 100 mW, the edge-to-edge spectral width of the output spectrum was broadened from 15 nm to 19 nm due to self-phase modulation effect. The corresponding center wavelength shifted by ~1 nm towards the short-wavelength direction. With the pump power at 100 mW, the autocorrelation trace was measured and shown in Figure 4-4(b). The pulse duration

(FWHM) is 35 ps, assuming a Gaussian profile. The time-bandwidth product is 83. As keep increasing the pump power, CW peaks appeared on the output optical spectrum and multiple-pulse operation was further observed.

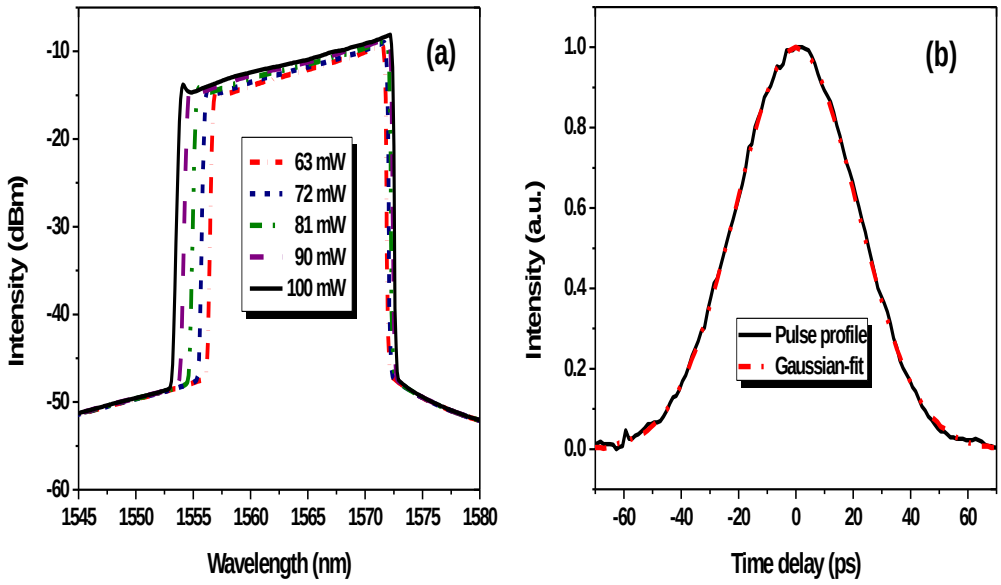

Figure 4-4 (a) Output optical spectra at different pump power. (b)Autocorrelation trace of the chirped pulse.

The variation of the output power as well as the corresponding pulse energy with the pump power was also measured, as shown in figure 4-5. It is clear that self-started mode-locking is achieved when the pump power is above a threshold value of 62 mW. Below 100 mW, our laser operated in a stable single pulse state with output average power up to 22 mW corresponding to calculated pulse energy up to 9.4 nJ. The laser will operate on the multi-pulse state as the pump power was increased above 100 mW. The spectral and the temporal widths of pulses became narrower once an additional pulse was generated, and then they became wider as the pump power increased [33]. It is necessary to mention that, a 1550 nm isolator was

employed external to the cavity in both the short and long cavity cases and, therefore, the unabsorbed 976 nm pump light was removed from the measured output signals.

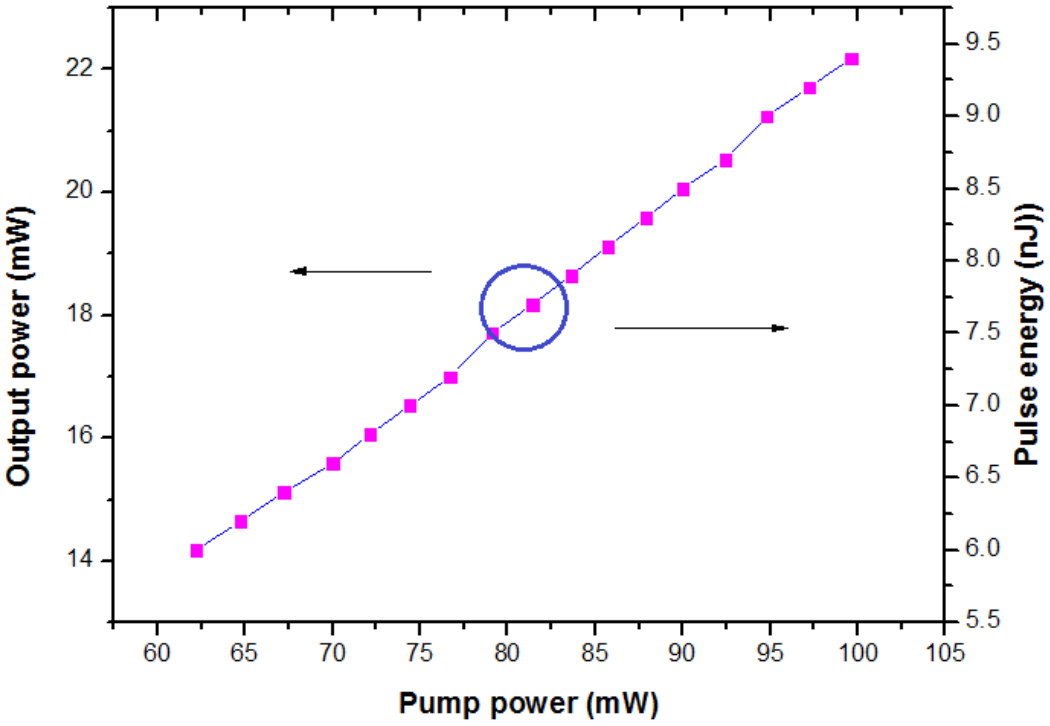

Figure 4-5: Pump power versus the output power and the corresponding output pulse energy.

It is shown that both the short and the long cavities output the pulses with strong chirp. To compress these highly chirped pulses, standard SMF was employed external to the cavities. For the short laser cavity, a 89-m-long SMF was proved to be a proper length by cut-back method to compensate the chirp accumulated inside the cavity and the output pulses can be compressed to ~300fs pulse width, 11% above the transform-limited pulse due to uncompressed nonlinear chirp, as shown in figure 4-6. In contrast to the short laser cavity, a 195-m-long SMF was used to compress the output pulses from the long laser cavity. The output pulses can be compressed to ~395 fs pulse width, see figure 4-6. The calculated time-bandwidth product is 0.53, 20% above the transform-limited profile indicating more nonlinear

chirp accumulated in the long cavity. It is clear from figure 4-6 that, both the compressed pulses have small satellites resulting from the nonlinear chirp of the pulse edges. The satellites for the short laser cavity case contain ~10% of the pulse energy while they contain ~20% of the pulse energy for the long laser cavity case. Both the chirp and the spectral width of pulses determine the length of SMF used to compress the output pulses. The larger the net cavity GVD and the narrower spectral width, the longer SMF is needed for pulse compression.

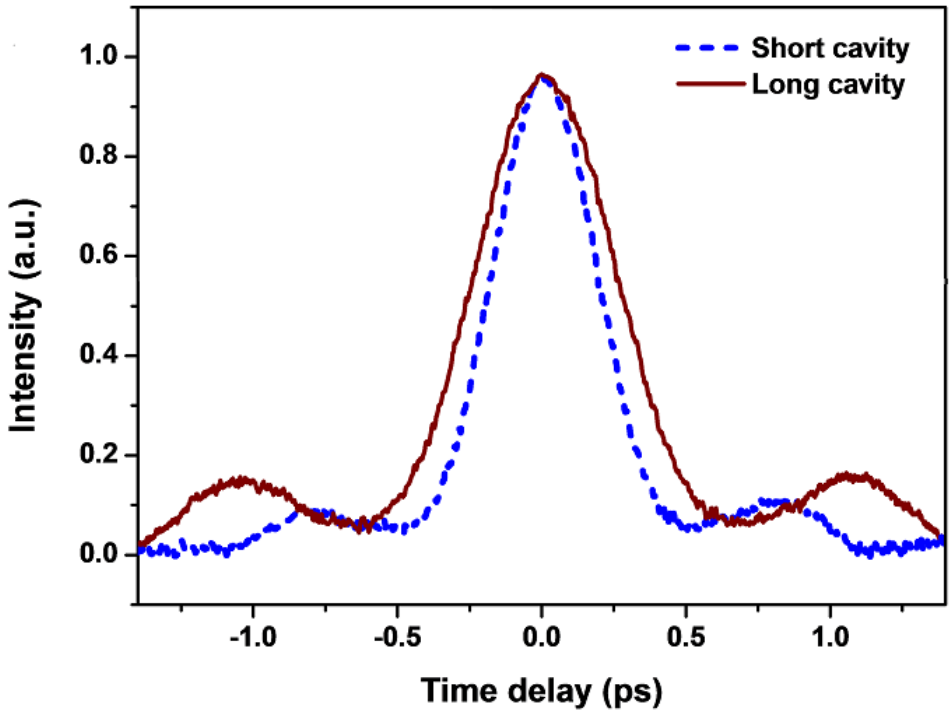

Figure 4-6 Dechirped pulses for two cavities

In the experiments, without inserting any additional spectral filter that was usually used in other large normal dispersion fiber lasers [34, 35], DSs with high pulse energies were realized in the proposed fiber lasers. That is because the pulse shaping in the large normal dispersion cavities is dominated by the limited gain bandwidth together with the gain saturation of the EDF. The EDF functioned as an

effective spectral filter. Experimental results showed that our lasers can operate stably more than two weeks. They can always self-start and get the same output characteristics when the pump power is above the threshold value.

In order to get insight into the laser stability, I also monitored the long term drift of the repetition rate of our long cavity laser. I define Δf as the drift of the repetition rate of the laser, namely, Δf=frep−firep, where frep is the instant repetition rate of the long cavity laser, and firep the initial repetition rate when the laser implemented self-started mode-locking. The repetition rate drift Δf within 1000min was measured using a signal-source analyzer (SSA, Rohde and Schwarz FSUP26) at a 10 Hz resolution bandwidth and 1 kHz span, as shown in figure 4-7(a). Clearly, in the early hours the repetition rate reduced slightly due to the thermal effect of the fibers within the cavity. The maximum drift is around 40 Hz, corresponding to the relative repetition rate variation of 1.7×10−5. Note that the duration of 1000min does not constitute any limit to the laser stability, but is merely the duration of the experiment. Additionally, the phase noise of the pulse trains from the long cavity laser was also characterized and presented in figure 4-7(b). In such an all-fiber laser design, technical noise influences are minimized and, therefore, quantum noise resulting from spontaneous emission in the amplification process dominates the phase noise [36]. Because of the wide pulse duration and large dispersion, the laser exhibits higher phase noise induced by quantum noise than soliton lasers. Calculation of the root mean square (rms) timing jitter is typically performed over a specified frequency band using the following equation

$$\Delta t_{rms} = \frac{1}{2\pi n f_{rep}} \sqrt{2\int_{f_L}^{f_H} S_n(f)\,df}$$

Equation 4-1[48]

where n denotes the harmonic order of the carrier measured, frep is the fundamental repetition rate of the pulse trains, and Sn(f) is the power spectral density of phase fluctuations per Hz. Here, fH and fL are boundaries of the frequency range. From equation 4-1, the integrated timing jitter between 10 Hz and 1 MHz is calculated to be 9.2 ps.

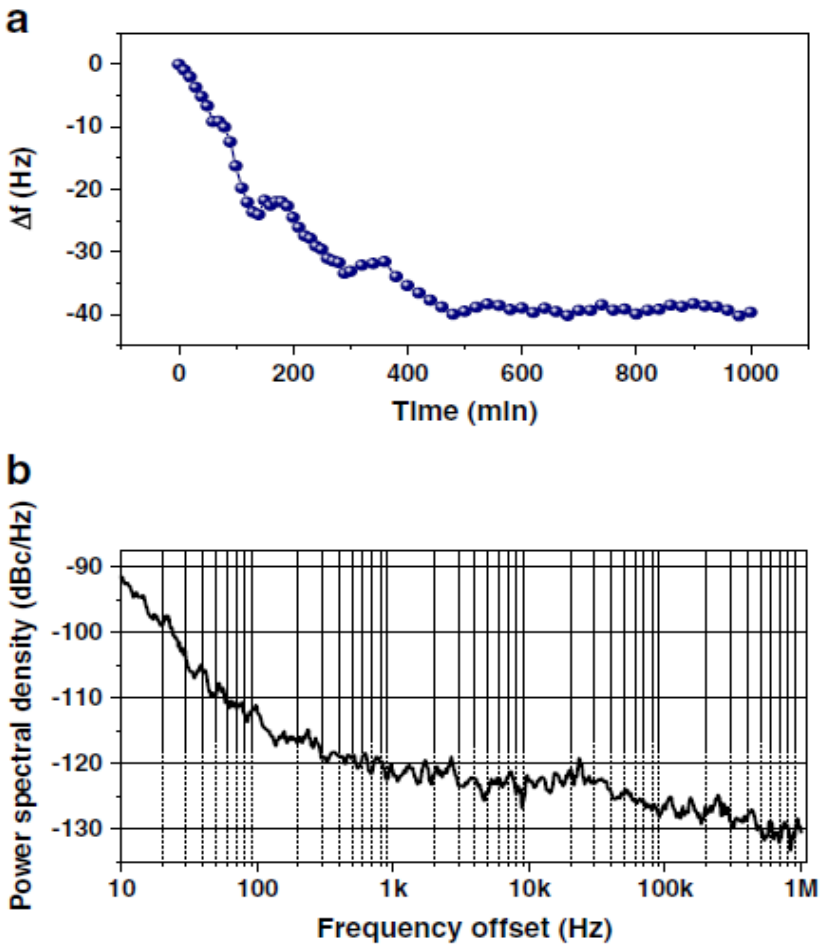

Figure 4-7. (a) Drift of the repetition rate and (b) Phase-noise power spectral density of the pulse trains of the presented laser.

4.4 Chapter summary

In this chapter, I have proposed an all-fiber-integrated DS EDF laser generating ultrashort high energy pulses. When the laser cavity is 25 m long, its pulse energies can be up to 5.9 nJ. The output chirped pulses are compressed to 300 fs in duration. In order to scale up the pulse energies, I have lengthened the cavity to 89 m by inserting a 64-m-long DCF within the cavity. Experimental results show that the pulse energies can be enhanced by 60% (up to 9.4 nJ) in this case. The output highly chirped pulses have duration of 35 ps and have been compressed to 395 fs. For the long cavity laser, its repetition rate drift as well as phase noise has also been investigated in the experiment.

Chapter 5 SWITCHABLE DUAL-WAVELENGTH MODE-LOCKING OF THULIUM-DOPED FIBER LASER BASED ON SWNTS

5.1 Introduction

Ultrafast light sources at 2 μm wavelength region have been widely investigated in recent years due to their eye-safe property, as well as their various scientific applications in the fields of remote sensing, nonlinear microscopy, medical treatment and free-space communication [37], [38]. Mode-locking is the most typical and commonly-used approach to generate ultrafast laser pulses. Different from active mode-locking techniques, passive mode-locking is simple, compact and low-cost without using active modulator in the laser cavity. Generally, passively mode-locked thulium-doped fiber lasers (TDFLs) can be implemented by nonlinear polarization rotation (NPR), nonlinear amplifying loop mirror (NALM) , nonlinear optical loop mirror (NOLM), semiconductor saturable absorber mirror (SESAM) , graphene, topological insulator, and the combination of saturable absorber (SA) with nonlinear switching based techniques .

As carbon allotropes draw much attention recently, single-wall carbon nanotube (SWCNT) has been demonstrated to possess ultrafast nonlinear optical responses.

By selecting the diameter of SWCNT, wide mode-locking operation has been realized over a wide wavelength range from 1 μm to 2 μm [39]-[41]. Compared to those lasers that are mode-locked at single wavelength, multi-wavelength mode-locked fiber lasers can simultaneously generate pulse-trains at different central wavelengths. Such type of lasers has attracted much interest as ultrafast laser technologies develop rapidly, and they can be used in next generation wavelength division multiplexing (WDM) transmission, optical signal processing, and precision spectroscopy. After literature review, numerous results are focus on multi-wavelength mode-locking in ytterbium-doped and erbium-doped fiber lasers [62], [63]. As for 2 μm wavelength region, a switchable dual-wavelength continuous wave (CW) fiber laser source has been demonstrated by a cascaded filter configuration [64]. However, such additional optical filter extends the cavity length and increases the implementation cost. NALM and NPR techniques, on the other hand, are good alternatives to obtain both mode-locking and filtering effect within the laser cavity to realize multi-wavelength mode-locking [65], [66]. Nevertheless, NALM-based and NPR-based mode-locking generally need high pump power and careful adjustment, in order to realize stable mode-locking operation.

5.2 Experimental Setup

Firstly, I prepare the SWCNT-based mode-locker using optically-driven deposition technique, which has been clearly reported in early works [42], [43]. The fabrication of the CNT-SAs utilizes the optically-driven deposition method. The movement of CNTs suspended in solution towards the connector end could be explained by thermophoresis, in which the temperature gradient is caused by

heating due to optical absorption [42]. The formation of CNTs in a ring pattern on the end-facet of the connector is believed to be a result of balancing between the scattering force and the gradient force generated by the optical radiation [42, 43]. Driven by a 20 dBm light source, the SWNTs are deposited on a standard FC/PC fiber end from dimethylformamide (DMF) solution. The inner ring diameter of self-fabricated SWNT is 14 μm. Since the optical field is mainly confined at the core of single mode fiber, our optically-driven deposition method with a larger inner ring diameter possesses much higher optical damage threshold, leading to high pump power injection as well as high-energy pulse generation [44], [45]. The modulation depth of the SWNT based mode-locker is 2.4%, and corresponding insertion loss is 1.7dB. The proposed fiber laser is schematically showed in figure 5-1. The SWNTs deposited on the surface of a standard FC/PC fiber connector to serve as a mode-locker. A 3.5 m commercial thulium-doped fiber (TDF, Nufern SM-TSF-9/125) is utilized as the gain medium, which is pumped via 1570/2000 nm WDM by an C+L band erbium-doped fiber amplifier (EDFA) with the capability of amplifying input signal to maximum output power of 5 W. The dispersion parameter of the used TDF is around 40 ps/km/nm at 2 μm wavelength. A 1570 nm CW laser with 1 mW output power is used as a seed source for optical amplification by such EDFA. The polarization of light is adjusted by a polarization controller (PC). The isolator is used to guarantee unidirectional propagation and to suppress detrimental reflections. A 10:90 fiber optical coupler (OC) is utilized as the output port of the fiber laser. All components within the cavity are fusion spliced, with a total cavity length of ~15 m. The net dispersion of the ring cavity is estimated to be ~-1.05 ps^2 at the operation wavelength of 2 μm, indicating of conventional soliton generation. An

optical spectrum analyzer (OSA, Yokogawa AQ6375) with a resolution of 0.05 nm is used to observe the optical spectra. Meanwhile, a real-time oscilloscope (OSC, Agilent 54641A) with a bandwidth of 350 MHz is used to monitor the repetition frequency with help of a photodetector (PD, EOT ET-5000F) of 12.5 GHz. Moreover, the radio-frequency (RF) spectrum is characterized by a signal source analyzer (R&S FSUP). Finally, the pulse profile is measured by a commercial autocorrelator (FR-103XL).

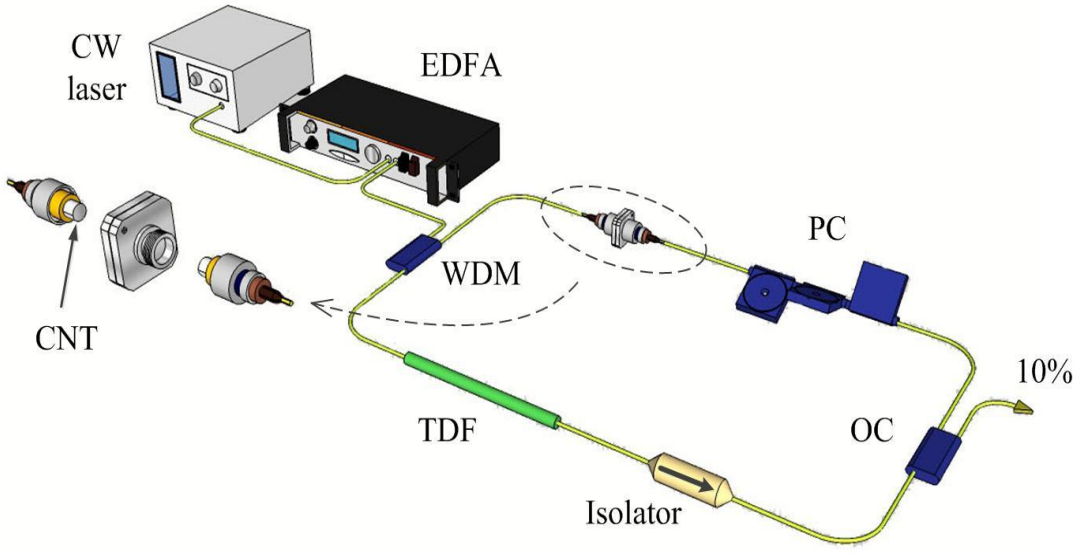

Figure 5-1. Experimental setup of mode-locked fiber laser

5.3 Experiment Results and Discussions

CW laser emission at central wavelength of 1947 nm is firstly observed, when the power of pump light is set above 200 mW. Once the pump power is further increased to 320 mW, self-started mode-locking at 1947 nm with an average output power of 3mW can be observed, as shown in figure 5-2. The blue line in figure 5-2. (a) presents the typical mode-locked spectrum with a 3-dB bandwidth of 2.2 nm. Spectral sideband is clearly observed, indicating that the TDFL is operated at the conventional soliton regime. The repetition frequency of the pulse-train is 13.6 MHz, corresponding to the cavity length of 15 m, as shown in figure 5-2. (b). The smooth peak intensity indicates that the fiber laser is operated with low amplitude noise. The inset shows the pulse profile with a pulsewidth of 2.8 ps, so that the pulse duration is 1.8 ps as the data is fitted by a sech2 profile. Therefore, the time-bandwidth-product (TBP) is ~0.32, indicating the pulse is almost transform-limited. Figure 5-2. (c) presents the RF spectrum with a scanning range of 200 MHz and a resolution of 1kHz. The background noise is lower than -90dBm. Meanwhile, the inset shows that the signal-to-noise ratio (SNR) of fundamental frequency is about 60 dB under the condition of 100Hz resolution. The corresponding background noise is about -100dBm. Therefore, the proposed 2 μm fiber laser with low amplitude noise is successfully verified by the smooth noise floor.

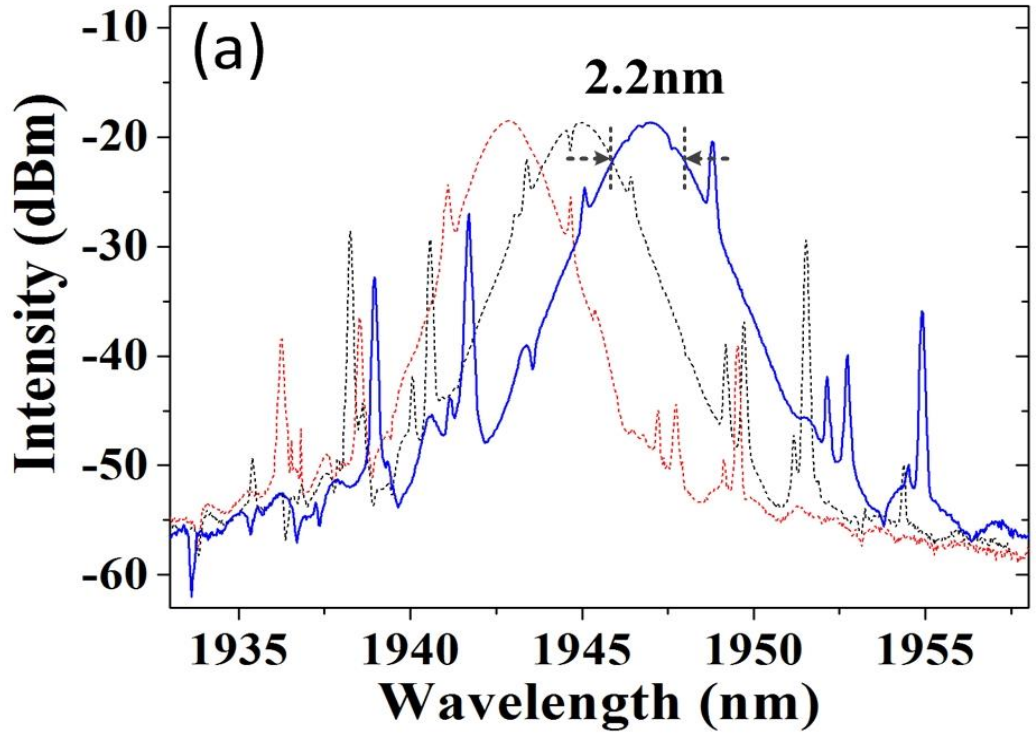
(a)
2.2nm
Intensity (dBm)
-10
-20
-30
-40
-50
-60
1935
1940
1945
1950
1955
Wavelength (nm)

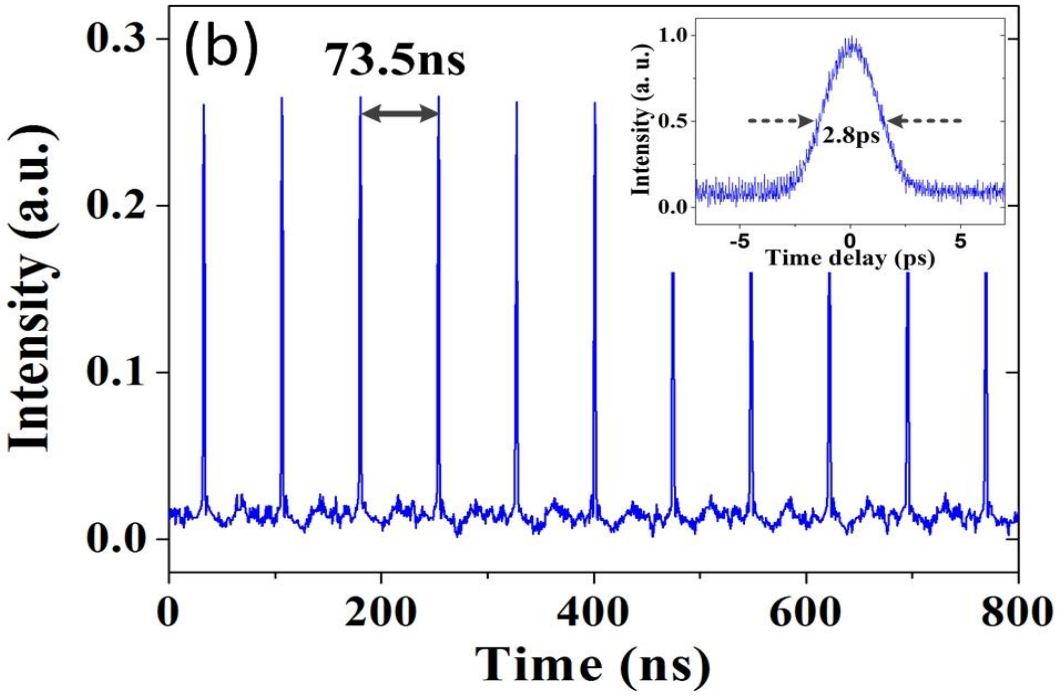
(b)
73.5ns
Intensity (a.u.)
0.3
0.2
0.1
0.0
0
200
400
600
800
Time (ns)
Intensity (a. u.)
1.0
0.5
0.0
2.8ps
-5
0
5
Time delay (ps)

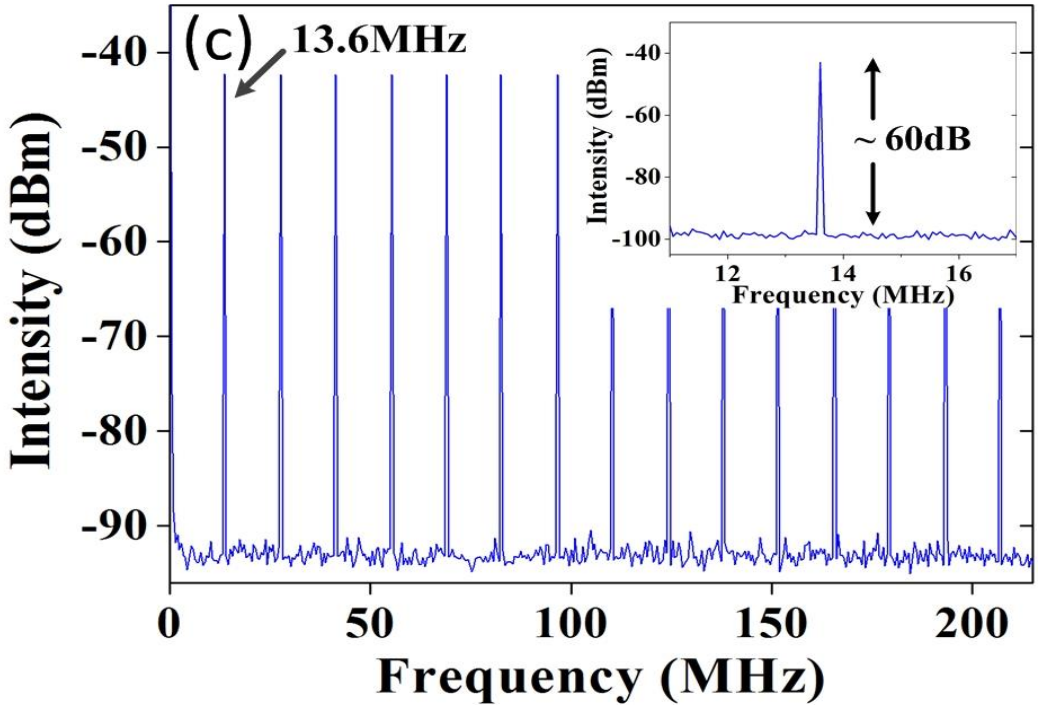

Figure 5-2. Wavelength-switchable mode-locking: (a) Optical spectra; (b) Oscilloscope trace of the pulse-train and autocorrelation trace (inset); (c) RF spectrum and fundamental frequency signal (inset);

Then, by adjusting the PC, the central wavelength of mode-locking can be switched to 1945 nm and 1943 nm, as shown in figure 5-2 (a) with black and red dash line. Especially, there is a tiny spectral dip at 1945nm, which does not move with the PC adjustment. I believe that such dip comes from one of the prominent water absorption bands at the wavelength of 1.94 μm [46]. In addition, the time-domain and frequency-domain features have no significant difference with results of 1947 nm. For the purpose of clear presentation, I ignore the corresponding characterization results.

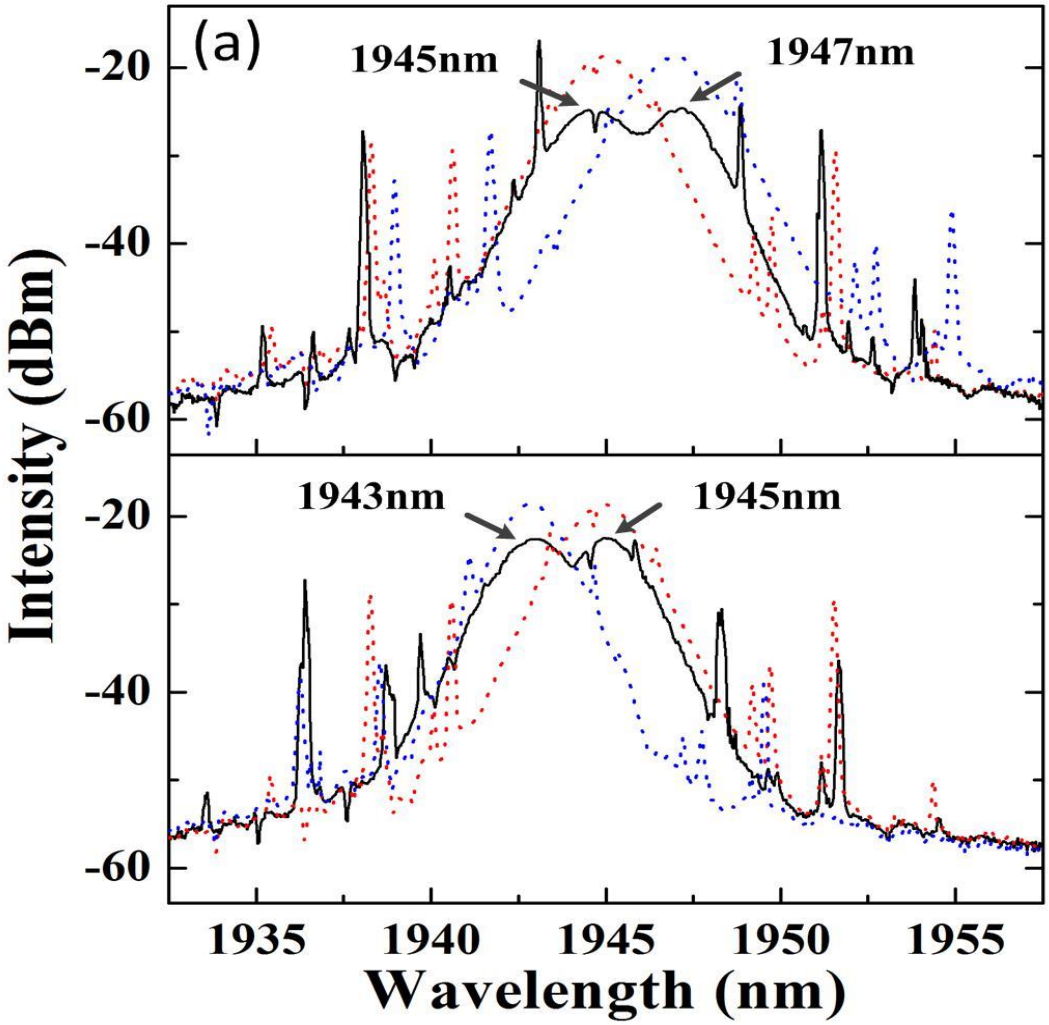
(a)
1945nm
1947nm
1943nm
1945nm
-20
-40
-60
-20
-40
-60
Intensity (dBm)
1935
1940
1945
1950
1955
Wavelength (nm)

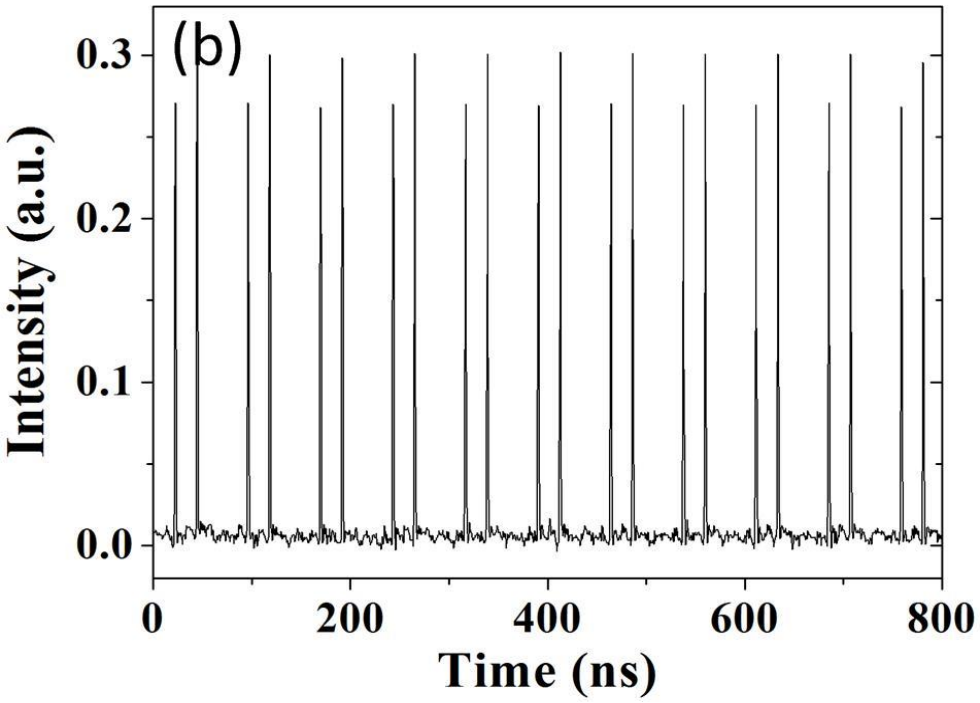

Figure 5-3. Switchable dual-wavelength mode-locking: (a) Optical spectra of 1945nm and 1947nm; (b) Optical spectra of 1943nm and 1945nm (c) Oscilloscope trace of the pulse-train.

When I further optimize the PC, a dual-wavelength mode-locking at both 1945 nm and 1947 nm can be obtained. If I further change to another optimal state of PC, another dual-wavelength mode-locking at both 1943 nm and 1945 nm can also be observed, as shown in Figure 5-3 (a). For the ease of comparison, optical spectra of single wavelength mode-locking for individual wavelengths are presented in Figure 5-3 (a) as well. I can conclude that optical spectrum of dual-wavelength mode-locking is a superposition of independent mode-locking at two wavelengths. Moreover, two dual-wavelength mode-locking results have almost the same peak power. In fact, the time-domain characteristics are similar as well. When I use the trigger function to stabilize one pulse-train, the other one moves randomly on the oscilloscope screen, indicating that two pulse-trains have different group velocities within the fiber ring cavity. Although two wavelengths have almost the same peak

power on the optical spectra, their peak intensities of two pulse-trains are not the same, as shown in Figure 5-3 (b). In addition, to investigate the long-term stability of such dual-wavelength mode locked TDFL, I continuously monitor its operation with one-hour interval for six hours under laboratory condition, as shown in figure 5-4. After six-hour performance monitoring by the OSA, the proposed 2 μm fiber laser has the wavelength drift of less than 0.05nm and spectral intensity fluctuation of less than 0.1dB at the peak wavelength. As for the dual-wavelength mode-locking operation, when I gradually reduce the pump power, it is found that only the spectral intensity becomes weaker, while the central wavelength and spectral bandwidth keep unchanged. Once the pump power is below the mode-locking threshold, CW laser emission at both wavelengths can be observed, as shown in Figure 5-5 (a) and (b). According to the CW emission spectrum, it is obvious that there exists an artificial comb filter inside the cavity, which is induced by the cavity birefringence [47].

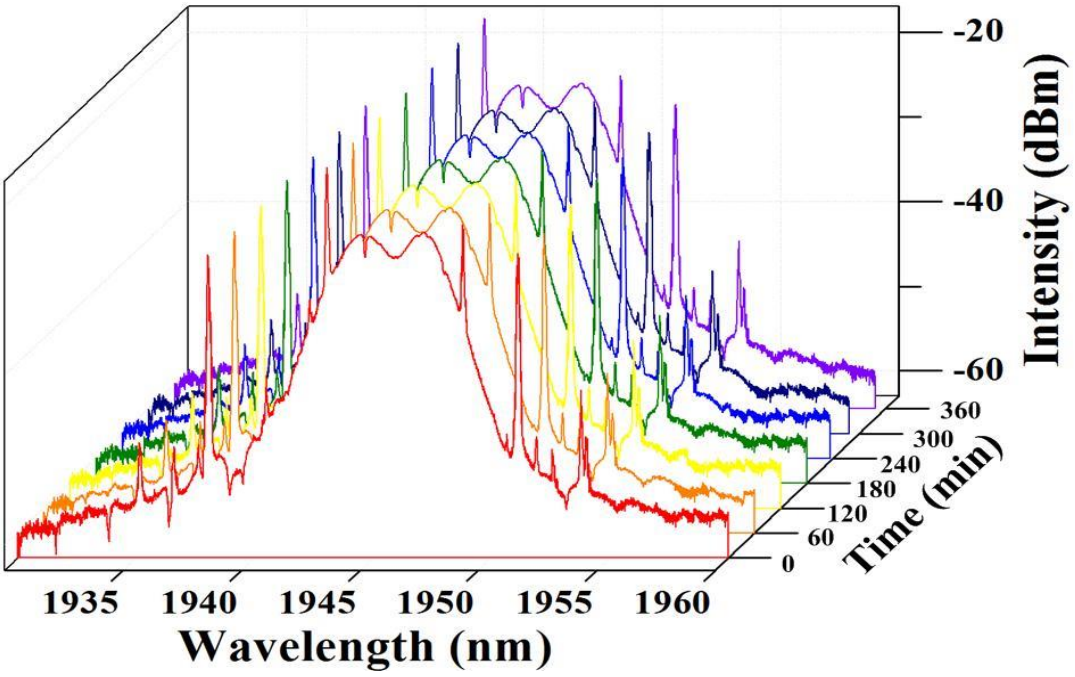

Figure 5-4. Long-term stability of dual-wavelength mode-locking.

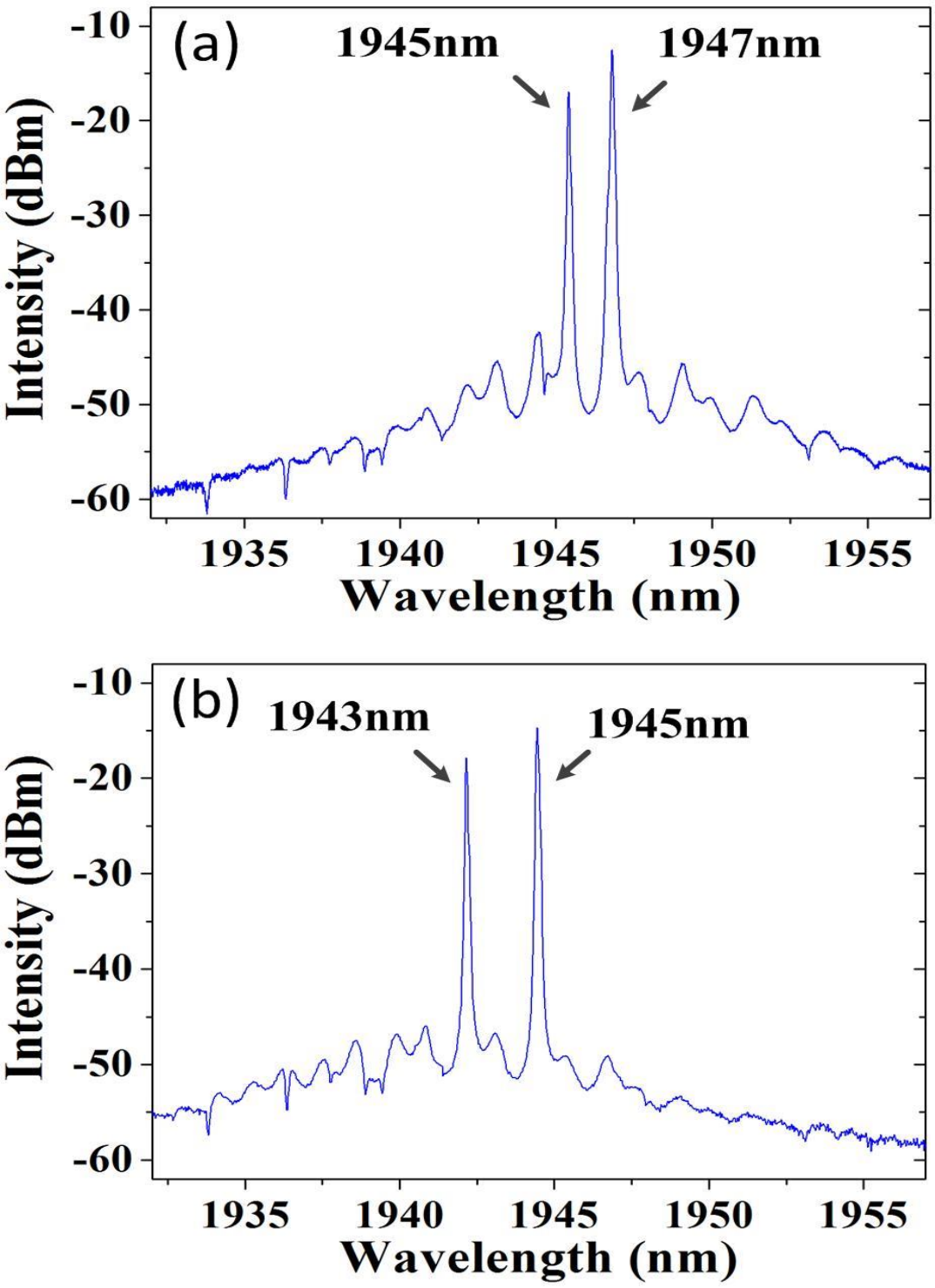

Figure 5-5. Spectra of dual-wavelength continuous wave emission: (a) 1945nm and 1947nm; (b) 1943nm and 1945nm

Next, I start to explore the effect of cavity birefringence. For our fiber ring cavity, no polarization sensitive component is used. However, after experimental characterization, I identify that the WDM component cannot be treated as polarization-insensitive. With the help of a fiber pigtailed polarization beam splitter (PBS), I find the polarization dependent loss (PDL) of the used WDM is around 3dB. Therefore, there exists weak nonlinear polarization evolution (NPE) effect in the fiber ring cavity, which is helpful to generate a tunable comb filter within the cavity and pave the way for multi-wavelength emission. In particular, once the SWNT is removed from the fiber ring cavity, only CW emission can be observed. Therefore, I can conclude that the NPE effect is not sufficiently strong to realize mode-locking. Instead, it only contributes to the tunable comb filter generation. In our experiment, by finely rotating the PC to perturb the cavity birefringence, the loss of different wavelengths varies. With the saturable absorption effect of the SWNTs, when two wavelengths have equal intensities and are both within the effective gain bandwidth range, dual-wavelength mode-locking operation is successfully obtained. If the cavity loss for one mode-locked wavelength is quite large while the others are relatively low, switchable individual mode-locking operation among 1943 nm, 1945 nm and 1947 nm can be obtained, respectively. According to the wavelength spacing of 2 nm, I can estimate the cavity birefringence to be 1.26×10-4. Since wavelength spacing is negatively related to the cavity birefringence, I can infer that triple or more wavelength mode-locking operation can be expected by strengthening the cavity birefringence, in case all wavelengths are within the effective laser gain range.

5.4 Chapter summary

In this chapter, I experimentally demonstrate a switchable dual-wavelength mode-locking TDFL using SWNTs as saturable absorber. Without any additional optical filters, I obtain a tunable cavity birefringence induced comb filter. By finely adjusting the intra-cavity birefringence, the proposed TDFL can be mode-locked not only at switchable single wavelength state, but also at switchable dual-wavelength state with long-term stability. These properties enable the advantages of compact size and flexible output, which make such TDFL a potential candidate for the molecular spectroscopy, optical communication, and biomedical applications.

Chapter 6 CONCLUSIONS

The aims of this PhD study are to design and construct passive mode locked fiber lasers at different wavelength and then analysis the application of passive mode locking based on different saturable absorbers. The satisfactory results show that I have fulfilled these tasks.

In chapter 3, I propose and demonstrate a wavelength-switchable passively harmonically mode-locked fiber laser with low pumping threshold using single-walled carbon nanotubes. When the pumping power of 980-nm laser diode is 60 mW, passive mode-locking (PML) of a soliton erbium-doped fiber laser at the 23rd harmonic of fundamental cavity frequency is experimentally observed at the central wavelength of 1530 nm. By only adjusting the polarization of laser in the cavity, another PML at the 13^{th} harmonic is successfully achieved at 1554 nm. The supermode suppression of each wavelength is larger than 30 dB. The pulses at 1530 nm are characterized in detail with a repetition rate of 328.44 MHz, a transform-limited pulse width of 1.3 ps, and a timing jitter of 142.6 fs.

In chapter 4, I experimentally demonstrate pulse energy enhancement in an all-fiber passively mode-locked laser operating in the large normal dispersion regime. By increasing the laser cavity length as well as its net cavity dispersion, the proposed laser, which is mode-locked by nonlinear polarization rotation, generates highly chirped dissipative solitons with pulse energies up to 9.4 nJ. The fundamental repetition rate is 2.3MHz, and the pulse duration is 35 ps. Such low repetition rate as well as wide pulse width makes this mode-locked all-fiber laser a suitable oscillator to directly seed a fiber amplifier, which can be used as compact sources for high-power applications.

In chapter 5, I experimentally demonstrate switchable dual-wavelength mode-locking of TDFL, using SWCNTs as SA. Due to the cavity birefringence-induced comb filter, switchable mode-locking can be individually realized for the proposed TDFL among three wavelengths of 1947 nm, 1945 nm, and 1943 nm, with almost the same 3-dB spectral bandwidth of 2.2 nm, repetition rate of 13.6 MHz and pulse-width of 1.8 ps. Furthermore, after finely adjusting the intra-cavity birefringence, I are able to demonstrate switchable dual-wavelength mode-locking at either 1947/1945 nm or 1945/1943 nm. The optical spectra of dual-wavelength mode-locking have almost the same characteristics and can maintain stable operation for a long period.

Publications

[1] K. Jiang, S. N. Fu, P. Shum, and C. L. Lin, “A Wavelength-Switchable Passively Harmonically Mode-Locked Fiber Laser With Low Pumping Threshold Using Single-Walled Carbon Nanotubes,” *IEEE Photon. Technol. Lett*., vol. 22, no. 11, pp. 754-756, Jun. 2010.

[2] K. Jiang, C.Ouyang, P.Shum, K.Wu, and J. H. Wong, “High-energy dissipative soliton with MHz repetition rate from an all-fiber passively mode-locked laser,” *Optics Communications*, vol. 285, pp. 2422-2425, 2012

[3] K. Jiang, Z.Wu, S. N. Fu, J.S, H. Li, M. Tang, P. Shum and D. Liu “Switchable Dual-Wavelength Mode-Locking of Thulium-Doped Fiber Laser Based on SWNTs” *IEEE Photon. Technol. Lett*., vol. 28, no. 19, pp. 2019-2022, Jun. 2016.

Bibliography

[1] Yuzo Ishida and Kazunori Naganuma, “Characteristics of femtosecond pulsesnear 1.5μm in a self-mode-locked Cr4+:YAG laser,” *Opt. Lett*, vol 19, pp. 1994.

[2] Fiber laser,http://en.wikipedia.org/wiki/Fiber_laser

[3] H. Haus, "A theory of forced mode locking," *IEEE Journal of Quantum Electronics*,, vol. 11, pp. 323-330, 1975.

[4] H. A. Haus, "Mode-locking of lasers," *Selected Topics in IEEE Journal of Quantum Electronics*, vol. 6, pp. 1173-1185, 2000.

[5] M. Hofer, M. H. Ober, F. Haberl, and M. E. Fermann, "Characterization of ultrashort pulse formation in passively mode-locked fiber lasers," *IEEE Journal of Quantum Electronics*, vol. 28, pp. 720-728, 1992.

[6] D. Kopf, F. X. Kärtner, K. J. Weingarten, and U. Keller, "Pulse shortening in a Nd:glass laser by gain reshaping and soliton formation," *Opt. Lett.*, vol. 19, pp. 2146-2148, 1994.

[7] K. Tamura, C. R. Doerr, L. E. Nelson, H. A. Haus, and E. P. Ippen, "Technique for obtaining high-energy ultrashort pulses from an additive-pulse mode-locked erbium-doped fiber ring laser," *Opt. Lett.*, vol. 19, pp. 46-48, 1994.

[8] F. X. Kärtner, D. Kopf, and U. Keller, "Solitary-pulse stabilization and shortening in actively mode-locked lasers," *J. Opt. Soc. Am. B*, vol. 12, pp. 486-496, 1995.

[9] U. Keller, K. J. Weingarten, F. X. Kartner, D. Kopf, B. Braun, I. D. Jung, R. Fluck, C. Honninger, N. Matuschek, and J. Aus der Au, "Semiconductor saturable absorber mirrors (SESAM's) for femtosecond to nanosecond pulse generation in solid-state lasers," *Selected Topics in IEEE Journal of Quantum Electronics*, vol. 2, pp. 435-453, 1996.

[10] L. E. Nelson, D. J. Jones, K. Tamura, H. A. Haus, and E. P. Ippen, "Ultrashort-pulse fiber ring lasers," *Applied Physics B: Lasers and Optics*, vol. 65, pp. 277-294, 1997.

[11] A. Tünnermann, J. Limpert, and S. Nolte, "Ultrashort Pulse Fiber Lasers and Amplifiers," in *Femtosecond Technology for Technical and Medical Applications*, 2004, pp. 35-54.

[12] P. U. Jepsen, R. H. Jacobsen, and S. R. Keiding, "Generation and detection of terahertz pulses from biased semiconductor antennas," *J. Opt. Soc. Am. B*, vol. 13, pp. 2424-2436, 1996.

[13] L. M. Zhao, D. Y. Tang, T. H. Cheng, H. Y. Tam, and C. Lu, "120nm Bandwidth noise-like pulse generation in an erbium-doped fiber laser," *Optics Communications*, vol. 281, pp. 157-161, 2008.

[14] L. B. Da Silva, K. Beop-Min, M. D. Feit, and A. M. Rubenchik, "Use of ultrashort pulse lasers in medicine," in *Lasers and Electro-Optics Society Annual Meeting, 1998. LEOS '98. IEEE*, 1998, pp. 443-444 vol.2.

[15] I. Hartl, X. D. Li, C. Chudoba, R. K. Ghanta, T. H. Ko, J. G. Fujimoto, J. K. Ranka, and R. S. Windeler, "Ultrahigh-resolution optical coherence tomography using continuum generation in an air?silica microstructure optical fiber," *Opt. Lett.*, vol. 26, pp. 608-610, 2001.

[16] H. N. Paulsen, K. M. Hilligse, J. Thøgersen, S. R. Keiding, and J. J. Larsen, "Coherent anti-Stokes Raman scattering microscopy with a photonic crystal fiber based light source," *Opt. Lett.*, vol. 28, pp. 1123-1125, 2003.

[17] C. L. Thomsen, D. Madsen, S. R. Keiding, J. Thogersen, and O. Christiansen, "Two-photon dissociation and ionization of liquid water studied by femtosecond transient absorption spectroscopy," *The Journal of Chemical Physics*, vol. 110, pp. 3453-3462, 1999.

[18] T. Udem, R. Holzwarth, and T. W. Hansch, "Optical frequency metrology," *Nature*, vol. 416, pp. 233-237, 2002.

[19] B. M. Kim, M. D. Feit, A. M. Rubenchik, and L. B. Da Silva, "Medical applications of ultrashort pulse lasers," in *Lasers and Electro-Optics, 1999. CLEO/Pacific Rim '99. The Pacific Rim Conference on*, 1999, pp. 43-44 vol.1.

[20] F.C. Dear, J.D. Shephard, X. Wang, J.D.C. Jones, D.P. Hand, "Pulsed Laser Micromachining of Yttria-Stabilized Zirconia Dental Ceramic for Manufacturing," *International Journal of Applied Ceramic Technology*, vol. 5, pp. 188-197, 2008.

[21] X. Liu, D. Du, and G. Mourou, "Laser ablation and micromachining with ultrashort laser pulses," *IEEE Journal of Quantum Electronics*, vol. 33, pp. 1706-1716, 1997.

[22] H. A. Haus, D. J. Jones, E. P. Ippen, and W. S. Wong, "Theory of soliton stability in asynchronous modelocking," *Lightwave Technology, Journal of*, vol. 14, pp. 622-627, 1996.

[23] W. E. Lamb, "Theory of an Optical Maser," *Physical Review*, vol. 134, p. A1429, 1964.

[24] J. M. DiDomenico, "Small-Signal Analysis of Internal (Coupling-Type) Modulation of Lasers," *Journal of Applied Physics*, vol. 35, pp. 2870-2876, 1964.

[25] L. E. Hargrove, R. L. Fork, and M. A. Pollack, "Locking of He-Ne Laser Modes Induced by Synchronous Intracavity Modulation," *Applied Physics Letters,* vol. 5, pp. 4-5, 1964

[26] C. J. Koester and E. Snitzer, "Amplification in a Fiber Laser," *Appl. Opt.,* vol. 3, pp. 1182-1186, 1964.

[27] L. F. Mollenauer and R. H. Stolen, "The soliton laser," *Opt. Lett,* vol. 9, pp. 13-15, 1984.

[28] H. Byun, D. Pudo, J. Chen, E. P. Ippen, and F. X. Kärtner, "High-repetition-rate, 491 MHz, femtosecond fiber laser with low timing jitter," *Opt. Lett,* vol. 33, pp. 2221-2223, 2008.

[29] J. R. Buckley, F. W. Wise, F. Ilday, and T. Sosnowski, "Femtosecond fiber lasers with pulse energies above 10 nJ," *Opt. Lett.,* vol. 30, pp. 1888-1890, 2005.

[30] A. Chong, W. H. Renninger, and F. W. Wise, "Route to the minimum pulse duration in normal-dispersion fiber lasers," *Opt. Lett.,* vol. 33, pp. 2638-2640, 2008

[31] C. K. Nielsen, and S. R. Keiding, "All-fiber mode-locked fiber laser," *Opt. Lett*. **32**(11), 1474-1476 (2007).

[32] Y. J. Song, M. L. Hu, C. Zhang, L. Chai, and C. Y. Wang, "High pulse energy femtosecond large-mode-area photonic crystal fiber laser," *Chinese Science Bulletin*, **53**(23), 3741-3745 (2008).

[33] X. M. Liu, and D. Mao, "Compact all-fiber high-energy fiber laser with sub-300-fs duration," *Opt. Express*, 18(9), 8847-8852 (2010)

[34] C. M. Ouyang, L. Chai, H. Zhao, M. L. Hu, Y. J. Song and C. Y. Wang, "Position Effect of Spectral Filter on Properties of Highly Chirped Pulses in an All-Normal-Dispersion Fiber Laser," *IEEE Journal of Quantum Electronics,* 45(10), 1284-1288 (2009).

[35] Y. Y. Zhang, C. Zhang, M. L. Hu, Y. J. Song, S. J. Wang, L. Chai, and C. Y. Wang, "High-energy subpicosecond pulse generation from a mode-locked Yb-doped large-mode-area photonic crystal fiber laser with fiber facet output," *IEEE Photon. Technol. Lett.,* 22(5), 350-352 (2010)

[36] H. A. Haus and A. Mecozzi, "Noise of mode-locked lasers," *IEEE J. Quantum Electron*., vol. 29, pp. 983–996, 1993

[37] M. E. Fermann and I. Hartl, "Ultrafast fibre lasers," *Nature Photon*., vol. 7, pp. 868-874, Nov. 2013.

[38] C. Xu and F. W. Wise, "Recent advances in fibre lasers for nonlinear microscopy," *Nature Photon*., vol. 20, pp. 875-882, Oct. 2013.

[39] A. Schmidt, S. Rivier, G. Steinmeyer, J. H. Yim, W. B. Cho, S. Lee, F. Rotermund, M. C. Pujol, X. Mateos, M. Aguilo, F. Diaz, V. Petrov, and U. Griebner, "Passive mode locking of Yb:KLuW using a single-walled carbon nanotube saturable absorber," *Opt. Lett*., vol. 33, no. 7, pp. 729-731, Apr. 2008.

[40] X. Zhao, Z. Zheng, L. Liu, Y. Liu, Y. Jiang, X. Yang, and J. S. Zhu, "Switchable, dual-wavelength passively mode-locked ultrafast fiber laser based on a single-wall carbon nanotube modelocker and intracavity loss tuning," *Opt. Express*, vol. 19, no. 2, 1168-1173, Jan. 2011.

[41] W. B. Cho, A. Schmidt, J. H. Yim, S. Y. Choi, S. Lee, F. Rotermund, U. Griebner, G. Steinmeyer, V. Petrov, X. Mateos, M. C. Pujol, J. J. Carvajal,

M. Aguilo, and F. Diaz, "Passive mode-locking of a Tm-doped bulk laser near 2 μm using a carbon nanotube saturable absorber," *Opt. Express*, vol. 17, no. 13, pp. 11007-11012, Jun. 2009.

[42] J. W. Nicholson, R. S. Windeler, and D. J. Digiovanni, "Optically driven deposition of single-walled carbon-nanotube saturable absorbers on optical fiber end-faces," *Opt. Express*, vol. 15, no. 15, pp. 9176-9183, Jul. 2007.

[43] K. Kashiwagi, S. Yamashita, and S. Y. Set, "In-situ monitoring of optical deposition of carbon nanotubes onto fiber end," *Opt. Express*, vol. 17, no. 7, pp. 5711-5715, Mar. 2009.

[44] K. Jiang, S. N. Fu, P. Shum, and C. L. Lin, "A Wavelength-Switchable Passively Harmonically Mode-Locked Fiber Laser With Low Pumping Threshold Using Single-Walled Carbon Nanotubes," *IEEE Photon. Technol. Lett*., vol. 22, no. 11, pp. 754-756, Jun. 2010.

[45] C. B. Mou, R. Arif, A. Rozhin, and S. Turitsyn, "Passively harmonic mode locked erbium doped fiber soliton laser with carbon nanotubes based saturable absorber," *Opt. Express*, vol. 2, no. 6, pp. 884-890, Jun. 2012.

[46] J. A. Curcio and C. C. Perry, "The Near Infrared Absorption Spectrum of Liquid Water," *J. Opt. Soc. Am*. A, vol. 41, no. 5, pp. 302-304, May. 1951.

[47] https://www.rp-photonics.com/mode_locking.html

[48] H.A. Haus, A. Mecozzi, "Noise of mode-locked lasers," *IEEE Journal of Quantum Electronics* 29 (3),983(1993)

[49] https://en.wikipedia.org/wiki/Laser

[50] D. J. Richardson, R. I. Laming, D. N. Payne, V. J. Matsas, and M. W. Phillips, "Pulse repetition rate in passive, selfstarting, femtmosend soliton fiber laser," *Electron. Lett*., vol. 27, pp. 1451–1452, 1991.

[51] A. B. Grudinin and S. Gray, "Passively harmonic mode locking in soliton fiber lasers," *J. Opt. Soc. Amer. B*., vol. 14, pp. 144–154, 1997.

[52] J. N. Kutz, B. C. Collings, K. Bergman, and W. H. Knox, "Stabilized pulse spacing in soliton lasers due to gain depletion and recovery," *IEEE Journal of Quantum Electronics*, vol. 34, no. 9, pp. 1749–1757, Sep. 1998.

[53] B. Ortac, A. Hideur, and M. Brunel, "Passive harmonic mode locking with a high power ytterbium-doped double-clad fiber laser," *Opt. Lett*.,vol. 29, pp. 1995–1997, 2004.

[54] F. Amrani, A. Haboucha, M. Salhi, H. Leblond, A. Komarov, P. Grelu, and F. Sanchez, "Passively mode-locked erbium doped double-clad fiber laser operating at the 322nd harmonic," *Opt. Lett*., vol. 34, pp. 2120–2123, 2009.

[55] Y. Deng, M. W. Koch, F. Lu, G. W. Wicks, and W. H. Knox, "Colliding pulse passive harmonic mode-locking in a femtosecond Yb-doped fiber laser with a SESAM," *Opt. Express*, vol. 12, pp. 3872–3877, 2004.

[56] K. Kieu and F. W.Wise, "Soliton thulium-doped fiber laser with carbon nanotube saturable absorber," *IEEE Photon. Technol. Le*tt., vol. 21, no.3, pp. 128–130, Feb. 1, 2009.

[57] J. W. Nicholson and D. J. DiGiovannni, "High-repetition-frequency low-noise fiber ring lasers mode-locked with carbon nanotubes," *IEEE Photon. Technol. Lett*., vol. 20, no. 24, pp. 2123–2125, Dec. 15, 2008.

[58] S. Y. Set, H. Yaguchi, Y. Tanaka, and M. Jablonski, "Laser mode locking using a saturable absorber incorporating carbon nanotubes," *J. Lightw. Technol*., vol. 22, no. 1, pp. 51–56, Jan. 2004.

[59] S. Zhou, D. G. Ouzounov, and F. W. Wise, “Passive harmonic modelocking of a soliton Yb fiber laser at repetition rates to 1.5 GHz,” *Opt. Lett.*, vol. 31, pp. 1041–1043, 2006.

[60] T. Hasan, Z. Sun, F.Wang, F. Bonaccorso, P. H. Tan, A. G. Rozhin, and A. C. Ferrari, “Nanotube-polymer composites for ultrafast photonic,” *Adv. Mater*., vol. 21, pp. 3874–3899, 2009

[61] N.B. Chichkov, K. Hausmann, D. Wandt, U. Morgner, J. Neumann, D. Kracht,” High-power dissipative solitons from an all-normal dispersion erbium fiber oscillator”*Opt. Lett* 35 (16) (2010) 2807.

[62] S. S. Huang, Y. G. Wang, P. G. Yan, J. Q. Zhao, H. Q. Li, and R. Y. Lin, “Tunable and switchable multi-wavelength dissipative soliton generation in a graphene oxide mode-locked Yb-doped fiber laser,” *Opt. Express*, vol. 22, no. 10, pp. 11417-11426, May. 2014

[63] Z. C. Wu, S. N. Fu, C. X, Chen, M. Tang, P. Shum, and D. M. Liu, “Dual-state dissipative solitons from an all-normal-dispersion Erbium-doped fiber laser: continuous wavelength tuning and multi-wavelength emission,” *Opt. Lett*., vol. 40, no. 11, pp. 2684-2687, Jun. 2015.

[64] S. Wang, P. Lu, S. Zhao, D. Liu, W. Yang, and J. Zhang, “2-$\mu\mu$m switchable dual wavelength fiber with cascaded filter structure based on dual-channel Mach-Zehnder interferometer and spatial mode beating effect,” *Appl. Phys*. B, vol. 117, no. 2, pp. 563-569, Jun. 2014

[65] Z. Y. Yan, X. H. Li, Y. L. Tang, P. P. Shum, X. Yu, Y. Zhang, and Q. J. Wang, “Tunable and switchable dual-wavelength Tm-doped mode-locked fiber laser by nonlinear polarization evolution,” *Opt. Express*, vol. 23, no. 4, pp. 4369-4376, Feb. 2015.

[66] W. J. Peng, F. P. Yan, Q. Li, S. Liu, T. Feng, and S. Y. Tan, “A 1.97 $\mu\mu$m multiwavelength thulium-doped silica fiber laser based on a nonlinear amplifier loop mirror,” *Laser Phys. Lett*., vol. 10, 115102, Sep. 2013.

[67] M. Guina, N. Xiang, A. Vainionpää, O. G. Okhotnikov, T. Sajavaara, and J. Keinonen, "Self-starting stretched-pulse fiber laser mode locked and stabilized with slow and fast semiconductor saturable absorbers," *Opt. Lett*., vol. 26, pp. 1809-1811, 2001

[68] J. Wu, D. Y. Tang, L. M. Zhao, and C. C. Chan, "Soliton polarization dynamics in fiber lasers passively mode-locked by the nonlinear polarization rotation technique," *Physical Review E,* vol. 74, 2006

[69] P. Urquhart, "Review of rare earth doped fibre lasers and amplifiers," *Optoelectronics, IEE Proceedings J,* vol. 135, pp. 385-407, 1988.